This is the accepted version of this paper. The version of record is available at https://doi.org/10.1016/j.compstruct.2021.114092

Impact characteristics of soft composites using shear thickening fluid and natural rubber-A review of current status

Amin Khodadadi[1], GholamhosseinLiaghat* [1, 2], Alireza Taherzadeh-Fard[1],Davoud Shahgholian-Ghahfarokhi[1]

* Corresponding author, Ghlia530@modares.ac.ir and G.Liaghat@kingston.ac.uk

[1]Department of Mechanical Engineering, TarbiatModares University, Tehran, Iran

[2] Department of Mechanical Engineering, Kingston University, London, United Kingdom

Abstract

The main focus of this review is on soft composites, relatively new to the literature. The ballistic fabrics, mechanism of ballistic energy absorption and parameters affect the ballistic performance of fabrics are reviewed. Adding shear thickening fluid (STF) and natural rubber (NR) to fabric and their potential to enhance the impact performance of woven fabrics are considered. Shear thickening mechanism, parameters influence the Shear thickening and impact response of fabric/STF composite are explored. Numerical modelling techniques for the estimation of impact resistance of fabric/STF are outlined. Also the role of shear thickening fluid in energy absorption of fabric/STF composite was investigated. Moreover mechanical and impact characteristics of elastomeric composites which contain one rubbery part as either matrix or completely separate media are explored as well, which have not been considered within previous review papers so far.

Keywords:Soft composite; Shear thickening fluid; Elastomer; Fabric/STF composite; Fabric/NR composite; Impact loading.

Contents

1. Introduction

Armors are mainly categorized into two types, namely hard armor and soft armor [1]. Hard armors have been used to protect against high-velocity projectiles. A complex process of fracture occurs during perforation of hard armor that have been investigated a lot during the last few decades [2-6]. Metals have been the primary materials used for ballistic applications due to the high hardness and tensile strength [2, 7, 8]. Ceramics armor systems are also widely used in ballistic applications [9-11]. While the main energy absorption mechanism of metallic armor is plastic deformation, in the case of ceramics, the main energy absorption mechanism is fracture. Ceramic armor systems consist of a layer of ceramic covered by high strength woven fabric such as Twaron, Dyneema, or Spectra [12]. Sandwich panels are also one of the important energy absorbers types which have complex and light structure. The panels have a light thick core made of different materials and shapes in the middle of the structure and two plates on both sides [13-16].

The three main armor's requirements are strength, flexibility, and weight. Although hard armors have high impact resistance capability, they are heavy and inflexible. On the contrary, soft armors or flexible armors are mainly used for body vests and protect from ballistic threats. It doesn't limit the wearer mobility. The material of soft armor are woven fabrics consist of high-strength fibers[17]. To meet the requirements mentioned above, many studies related to ballistic fabrics and composites have been done in the past two decades [18-21]. Impact resistance mechanisms and characteristics of such materials have been investigated a lot by numerical and experimental methods [22, 23].

Recently, some research have been conducted to study different approaches of ballistic fabrics impact resistance improvement. Shear thickening fluid (STF) has

attracted attention due to its special properties when subjected to impact loading [24]. STFs are composed of dense suspension of nanoparticles in a fluid. This fluid is characterized by remarkable increase in viscosity when the applied shear rate exceeds a critical value [24]. Adding STF to fabric enhance the soft body armor impact resistance[25]. Another approach used by researchers is coating the fabrics with natural rubber. Using rubber material is a new approach to improve the ballistic performance of fabrics which results in soft composite target. Rubber materials have been widely used in impact resistance panels, shock absorbers, and other engineering applications [26, 27]. Besides, high flexibility [28] and high damping properties [29] make rubber matrix composites a suitable material for ballistic and blast applications.

This paper aims to review the impact characteristic of soft targets. Woven fabrics made of high-performance fibers are considered in this paper. Fabric energy absorption is dependent on some factors such as material properties, fabric structure, projectile geometry, friction, and pre-tension and therefore, these factors are reviewed in this study. Furthermore, fabrics reinforced with STF for developing soft composite targets will be discussed. The rheological properties of STFs and mechanisms of shear thickening phenomenon will be considered. The ballistic performance of STF impregnated fabrics will also be discussed to provide better understanding of STFs in these applications. Reinforcement of woven fabrics with natural rubber will be studied and ballistic performance of rubber-coated fabrics will be reviewed. In the final section, using rubber as a layer in a laminate is studied and mechanical properties and impact response of laminates in presence of elastomer layer will be discussed.

2. Impact response of fabric panels

It has been proved that high-performance fiber-woven fabrics containing, for example, ultra-high-molecular-weight polyethylene (UHMWPE), and aramid, exhibit satisfactory velocity impact load resistance. The purpose of this section is to review ballistic fabrics, the fundamental ballistic energy dissipation mechanism, and the factors that are involved in ballistic fabric energy absorption, e.g., fabric structure, material properties, the geometry of the projectile, pre-tension, and friction.

2.1.Ballistic Fabrics

High performance fiber-woven fabrics have been employed in a large number of applications. Many studies investigated improving the impact response of such fabrics [30-32]. In the molecular structures, aramid fibers exhibit extremely high primary and secondary bond strength. They also enjoy significant impact resistance. As a result, researchers have exploited aramid fabrics in soft armor fabrication to obtain great toughness, modulus, and strength[33, 34]. A number of aramid-based materials are employed for ballistic purposes, including Kevlar and Twaron[35-38]. They provide several advantages such as a high melt point, flexural strength, satisfactory abrasion, creeping/fatigue resistance, and a light weight [39]. However, the disadvantages of aramid-based materials include treatment and processing difficulties, small compressive strength, and rather large moisture absorbency.

Additionally, considering their great strength, light weights, and good flexibility, there is an increasing tendency to utilize aramid fibers and ultra-high-molecular-weight polyethylene (UHMWPE) [40, 41]. The advantages of UHMWPE include a low melting point and no water absorption. Spectra and Dyneema UHMWPE products are employed for commercial-scale ballistic purposes. In contrast to UHMWPE, the biological and chemical agent resistance of aramid-based materials is not high [42]. Furthermore, as a

rigid-rod polymer sub-class, poly(p-phenylene2,6-benzobisoxazole) (PBO) provides great ultimate tensile strength and modulus of elasticity [43, 44]. Ballistic researchers treat PBO to be a substitute for Kevlar. Although they enjoy significant tensile strength, PBO have poor transverse bonds, shear modulus, and shear strength. Also, PBO has a small compressive yield point and undergoes moisture degradation [45].

2.2.Mechanism of ballistic energy absorption

The primary yarns of a woven fabric engage projectile when they are subjected to a projectile strike, absorbing most of impact-induced kinetic energy. The primary yarns that undergo transverse deflection pull the secondary yarns that are not in direct projectile contact. Longitudinal and transverse waves are propagated by the secondary yarns, helping the primary yarns drive longitudinal and transverse waves in the adjacent yarns. The secondary yarns are absorptive of solely a portion of the projectile kinetic energy on account of the transverse deflection, which continues to rise until the impact point strain leads to breakage [46].

From the perspective of energy transfer, one can say that a combined mechanism consisting, for example, primary yarn tension, fabric deformation, frictional yarn/projectile slipping, yarn/fabric pullout, and the breakage of yarns dissipates the impact kinetic energy of a projectile-fabric collision [47, 48]. A Kevlar fabric failure study was conducted by Manimala and Sun [49]through indentation tests in quasi-static settings. They found that the sliding and breakage of yarns were the most prominent factors in the absorption of energy. Tabiel and Nilakantan[50] observed that the molecular-level bond rupture and the bowing and pullout of yarns served as energy dissipation mechanisms. Likewise, Nilakantan et al. [51] found the sliding and pullout of yarns to be the primary energy dissipation modes. Shaktivesh and

Naik[48]analytically formulated fabric targets under ballistic impacts. They incorporated mechanisms of damage. Energy absorption was reported to occur through yarn tension, target compression under the projective, impact zone compression, conical deformation, shear plugging, in-plane yarn friction, and projectile-fabric thickness friction.

2.3.Factors influencing ballistic performance of fabric panels

Tabiei and Nilkantan[50], Cheeseman and Bogetti[52] and Mawkhlieng and Majumdar[53]suggested that several parameters are involved in fabric ballistic performance. They analyzed such parameters in terms of their effects on woven-fabric ballistic performance. The factors that influence ballistic fiberperformance are highlighted below.

2.3.1. Material properties

The elasticity modulus and tensile strength of yarns have substantial effects on woven fabric ballistic performance. Higher impact-induced kinetic projectile energy could be absorbed by yarns that have larger fracture strains and tensile strength. Smith et al. [54] argued that the density and modulus of yarns determine the speed of longitudinal stress waves propagating through yarns. The yarn modulus can be obtained as

$$C = \sqrt{E/\rho} \qquad (1)$$

As can be seen, a larger modulus leads to a larger propagation speed of waves through yarns. Thus, a larger number of yarns contribute to the absorption of energy, enhancing the dissipation of energy due to the quicker transmission of stresses and strain to the secondary yarns. Rao et al. [55] numerically modeled the ballistic behavior of woven fabrics to explore the corresponding influences of the strength and

longitudinal elasticity modulus of yarns. They observed that greater stiffness resulted in a larger reduction rate of the projectile speed. However, large yarn strength enabled yarns to undergo larger deformation prior to rupture, leading to greater projectile kinetic energy absorption, as illustrated in Fig. 1.

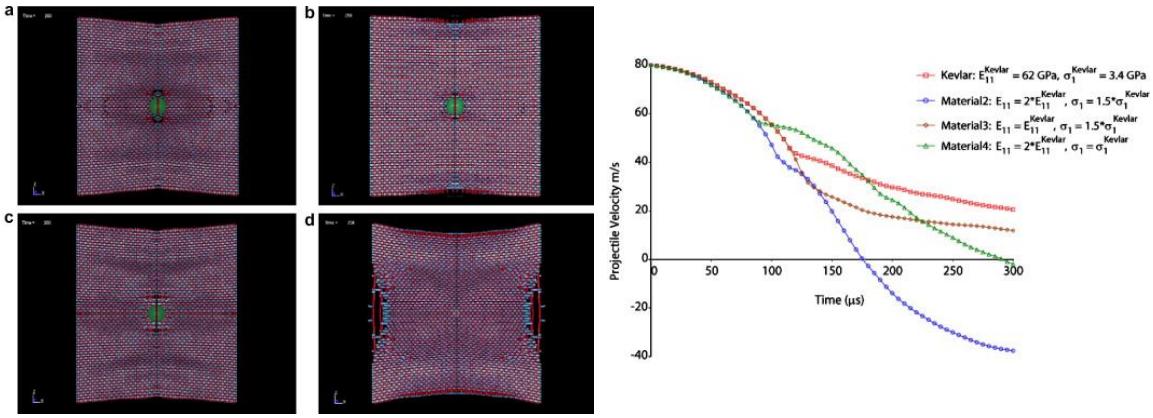

(i) (ii)

Fig. 1 (i) Back face damage of fabrics at V_s = 80 m/s. (a) Baseline Kevlar fabric at 200 μs after impact. (b) Fabric with Material2 yarns at 250 μs after impact. (c) Fabric with Material3 yarns at 200 μs after impact. (d) Fabric with Material4 yarns at 250 μs after impact (ii) The projectile velocity time history for impact on different material properties fabrics [55]. Reprinted with permission from ref. 55 (Copyright © 2009 Elsevier).

Despite the fact that a larger longitudinal elasticity modulus induces a greater reduction rate of the projectile speed, an excessively large longitudinal modulus would result in a premature primary yarn failure and fabric perforation, even when the impact velocity is low [31].Research has demonstrated Poisson's ratio to have no effects on fabric impact resistance [56]. This is also the case with the transversal elasticity modulus. A low transverse modulus could sometimes induce early damage of yarns [56].

Statistical yarn tensile strength distribution is a source of variable influencing the impact performance of yarns. Nilakantan et al. [57] performed numerical simulations to explore the influence of the statistical strength distribution of yarns on the probabilistic impact responses of fabrics by five strength distribution scenarios with

different widths and strengths. They observed the strength distribution of yarns to be a considerable factor in probabilistically determining the penetration behavior of fabrics. Overall, the modulus and tensile strength of yarns could be claimed to have the most considerable effects on fabric ballistic behavior.

2.3.2. Fabric structure

Two-dimensional woven fabrics are frequently employed for ballistic purposes to cope with different threat types, such as projectile impacts. Such fabrics consist of two sets of orthogonal yarns, i.e., the warp (0º) and weft (90º) yarns. These orthogonal sets are woven into each other to create the surface of the fabric. Satin, knitted, twill, basket, and plain weaving configurations are the basic weaving systems [39]. Previous studies explored the influences of woven structures on the impact resistance of fabrics, improving plain weaving in comparison to satin, twill, and basket patterns [58, 59]. Furthermore, interlayer friction properties could be affected by various patterns of weaving [60]. Tran et al. [61]analyzed three commonly-used two-dimensional composite fabrics, i.e., knitted, basket, and plain weaving patterns, in terms of impact performance and damage under the penetration of a projectile. The knitted pattern exhibited the lowest resistance. The impact performance of the basket pattern was found to be similar to the knitted one, with higher fabric flexibility than plain-woven fabric rigidity. Yang et al. [62]studied the satin, twill, and plain weaving patterns when subjected to impact loads. Fig. 2 illustrates the velocity evolution of projectiles. As can be seen, at an initial projectile velocity of 200 m/s, the residual velocities were all in a narrow range of 176-179 m/s and had similar profiles of evolution. In contrast to Tran et al. [61], the basket and satin weaving patterns exhibited the largest and smallest absorption of energy, respectively. It should be noted that the weaving patterns and

firmness of fabrics have larger effects on the overall performance of single-ply system than multi-ply ones[62].

Apart from the aforementioned weaving patterns, cellular patterns are produced by the end-to-end placement of the warp and weft yarn floats so that protruding and indenting cellular configurations could be obtained on the surface of the fabric. Cellular waving patterns undergo perforation under larger loads and experience greater deformation as compared to plain weaving patterns since the end-to-end-placed side-by-side-aligned warp and weft yarn floats can withstand projectiles. Thus, a cellular-woven fabric has good flexibility and strength in the perpendicular direction to the surface of the fabric [63].

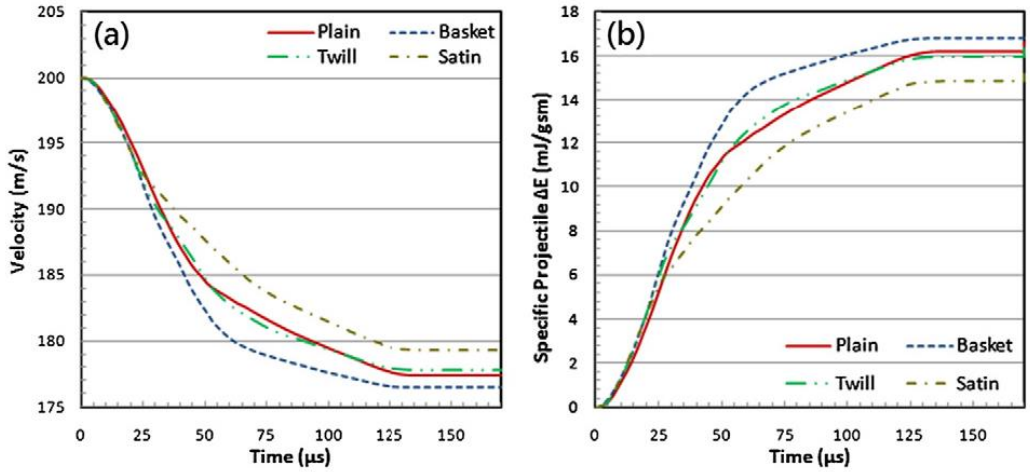

Fig. 2 Multi-layer evolution of: (a) The projectile velocity time history, (b) specific projectile ΔE [62]. Reprinted with permission from ref. 62 (Copyright © 2015 Elsevier).

Given the focus of the aforementioned studies on two-dimensional plain-woven fabrics, there is a lack of sufficient data on the ballistic impact performance of three-dimensional theoretical and experimental woven fabric models [64-66]. A three-dimensional fabric structure is created by the connection of a number of two-dimensional layers through layer interlaces via out-of-plane direction z-tows/yarn or two-dimensional layer stitches at specific crossovers [59]. In general, one can divide

three-dimensional warp fabrics into two major categories based on the number of fabric-traveling warp weavers. Warp weavers passing throughout thickness are known as through-thickness interlocks, as shown in Figs. 3a and 3b. However, warp wavers there are solely two filling layer bonds in layer-to-layer structures, as illustrated in Fig. 3c. Also, the interlacing angle-based classification of warp fabrics is possible. The first category is the interlock angle at which interlacing could be performed at all degrees, except for 90°, as shown in Fig. 3b. The second category refers to a particular case of the first category. An interlacing angle of 90° leads to an orthogonal interlock, as shown in Fig. 3a -the x- and y-yarns of the orthogonal structures and angle-interlock. However, in a full interlacing setting, the x-yarns undergo interlacing with not only the y-yarns but also the z-yarns, as demonstrated in Fig. 3d [67, 68].

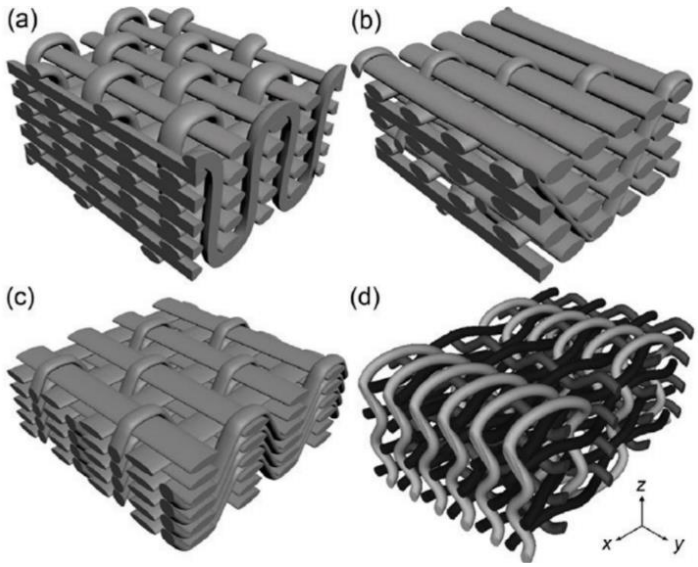

Fig.3 3D woven structures: (a) orthogonal, (b) through-the-thickness angle interlock, (c) layer-to-layer angle interlock, and (d) fully interlaced [68]. Reprinted with permission from ref. 68 (Copyright © 2017 IntechOpen).

Three-dimensional fabrics provide significant advantages over plain-woven ones, including greater interlaminar properties and through-thickness. Such fabrics resist impact loading in three orthogonal directions rather than in two planar directions. This adds to their ability to absorb energy [69, 70].

2.3.3.Friction

Inter-yarn friction is a primary mechanism of energy absorption within soft body armor [71-73]. Different fabric weaving patterns were investigated by Briscoe and Motamedi[74] at three inter-yarn friction coefficients. It was observed that fabric perforation requires a larger projectile velocity at a larger inter-yarn friction coefficient. However, a reduction in the inter-later friction coefficient raised the residual projectile velocity – that is, larger fabric energy absorption occurred at a greater inter-layer friction coefficient. Friction coefficient alternation is a technique to study the effects of friction on fabric ballistic performance. Bazhenov et al.[75]analyzed the effects of water on fiber pullout and indentation forces by pullout tests. Water was found to alternate the friction forces and pullout character of fibers. Then, fabrics may undergo substantial behavior changes under impact loading. As an important finding, larger inter-yarn friction cannot be confidently said to exhibit higher ballistic performance. In fact, a change above a certain level in the friction coefficient could pose a negative effect on the failure mechanism and energy dissipation. A friction coefficient above the critical quantity makes the over-constraint movement of yarns more likely. This would diminish the absorption of energy and adversely influence ballistic performance [76, 77]. The influences of friction were numerically examined by Wang [78]. They incorporated several friction coefficients, evaluating fabric ballistic performance, as shown in Fig. 4. It was observed that a rise in the friction coefficient to 0.7 enhanced fabric energy absorption in various inter-yarn friction conditions. A further increase in the friction coefficient began to diminish the absorption of energy. Furthermore, the yarn surface stress has been demonstrated to be sensitive to crossing yarn friction. A rise in the yarn friction coefficient decreases the stress at the fabric-projectile contact edge. Larger

inter-yarn friction in fabrics increases the fabric penetration time of a projectile, in comparison to fabrics with smaller inter-yarn friction [78]. In addition, the projectile nose has been proved to have a small effect on the failure mechanism at greater friction [79].

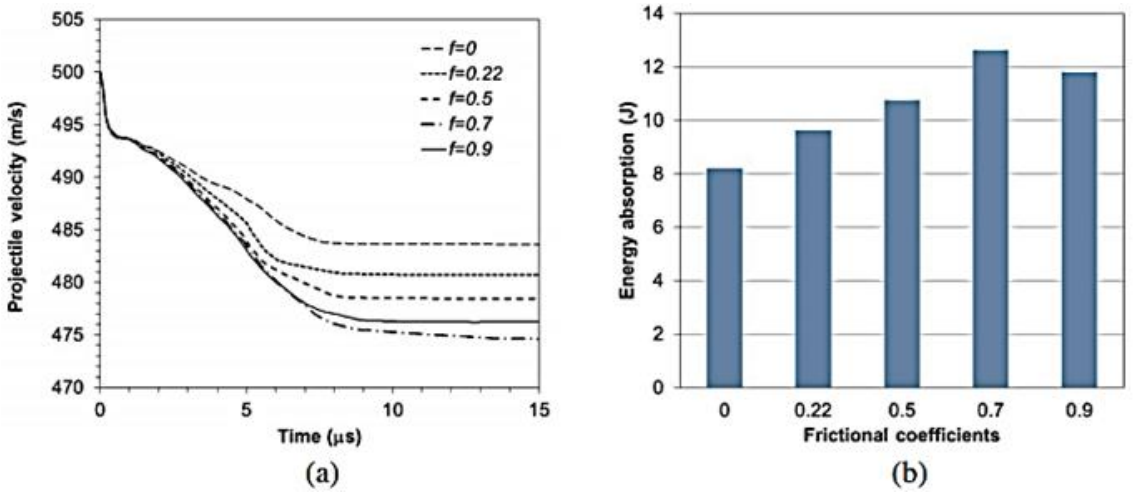

Fig. 4 Schematic of (a) projectile velocity with different frictional coefficients (b) energy absorption with different frictional coefficients [78]. Reprinted with permission from ref. 78 (Copyright © 2016 Elsevier).

2.3.4.Projectile geometry

The geometry of a projectile is an essential parameter that affects the responses of woven fabrics to ballistic impacts. Different sizes and shapes of projectiles are available. Also, the projectile nose may range from smaller than the width of a single yarn to that of numerous yarns. The characteristics of projectiles, including the impact velocity, mass, shape, and size, determine woven fabric ballistic performance. For the overall impact performance evaluation of fabrics, it is required to combine such characteristics and other impact features [80]. The effects of projectile features on the response of full-clamping one-layer plain-woven Kevlar fabrics were analyzed by Nilakantan et al. [81]. They employed conical, cylindrical, and spherical projectiles with equal impact velocities and weights. It was found that the conical projectile had the capability of easy penetration in the fabric since a conical projectile would tend to

"window" or push aside the principal yarns. The six projectiles along with the velocity history after impacting the target are shown in Fig. 5. As can be seen, the fabric was able to stop solely larger cylindrical projectile. The fabric was penetrated by the remaining projectiles, and the residual velocities of the projectiles reduced in the order of the small conical, small spherical, small cylindrical, and large spherical projectiles.

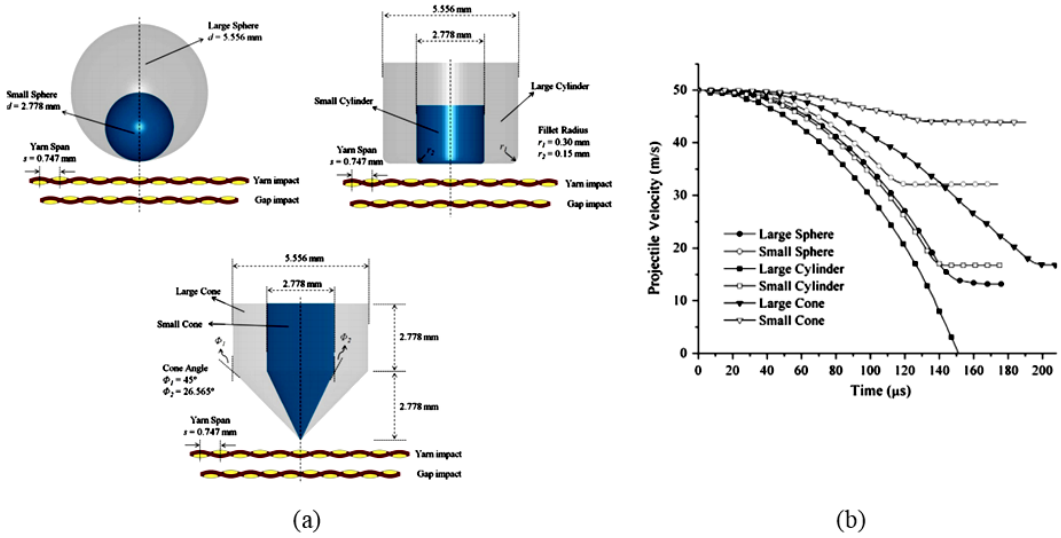

Fig. 5 (a) Spherical, cylindrical, and conical projectile (b) projectile velocity time histories [81]. Reprinted with permission from ref. 81 (Copyright © 2013 Elsevier).

Concerning conical projectiles, the relationship between the nose angle of a conical projectile and the impact magnitude and penetration size was evaluated by Talebi et al. [82] on fabrics with high strength. As can be seen in Fig. 6, the nose angles of 30-60 degrees were incorporated. A realistic yarn-level fabric model was fabricated, performing numerical impact simulations for various projectiles. Fig. 6 plots projectile energy absorption versus the nose angle. As can be observed, the absorption of energy may be divided into four zones. Zone 1 contains fabric wedging as the dominant failure mode. At an angle of 60-105 degrees, the fabric failure mechanism shifts from wedging to shear (Zone 2). In Zone 3, shear is the dominant mechanism of failure, with a larger number of yarns breaking. Eventually, Zone 4 involves a sharp shift in the absorption of

energy by a change in the nose angle. At this point, the nose of the projectile leads to maximum yarn breakage, which is possible, and fabric perforation. Also, earlier studies analyzed the influences of projectiles with non-conventional shapes, e.g., a high-carbon steel razor blade, fragment simulation projectiles (FSP), and rounded-head projectiles[83].

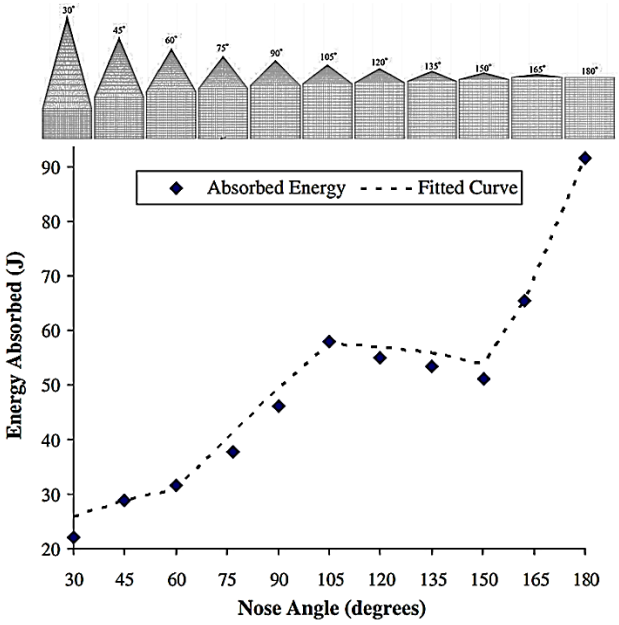

Fig. 6 Energy absorption of projectiles with different nose angle [82]. Reprinted with permission from ref. 82 (Copyright © 2009 Elsevier).

2.3.5. Pre-tension

Research has recently examined the relationship between woven fabric ballistic performance and pre-tension. Pre-tension reduces the mobility of yarns and the capacity of fabric strains to absorb energy; however, it enhances fabric stiffness and stress propagation. As a result, pre-tension raises the number of deformation-involved yarns. Thus, an initial pre-tension level increases the ballistic limit; however, a rise in pre-tension beyond the critical level would decrease the ballistic limit [84]. Lulu et al. [85]studied the impact behavior of multi-layered Kevlar 49 woven fabrics under fan blade-out. The tensile loads of 25, 50, and 75 N were applied using a tension control

winding system. They approximated the residual projectile velocity through high-speed photographs. It was found that the specific fabric energy absorption initially underwent a rise but then substantially declined as the pre-tension of the fabric increased. The medium specific energy absorption was 7.53-9.47 $kJ.g^{-1}.cm^2$ at a tensile load of 25 N. However, a pre-tension load of 50 N would raise the specific fabric energy absorption to up to 10.8 $kJ.g^{-1}.cm^2$. The smallest specific pre-tensioned fabric energy absorption occurred to be 6.67-7.3 $kJ.g^{-1}.cm^2$ at a larger pre-tension load (i.e., 75N). This implies that a rise in the pre-tension load above the optimal quantity would not enhance containment fabric settings in terms of ballistic performance.

Additionally, a rise in the pre-tension of fabrics would raise the pullout load [86]. At smaller pre-tension loads of fabrics, larger pullout loads were observed in the warp yarns than in the fill yarns. At larger pre-tension loads, on the other hand, higher uniformity was observed in the pullout loads of the fill and warp yarns. This stems from a greater crimp of the warp yarns than that of the fill ones in non-tensioned fabrics. As can be seen in Fig. 7, a rise in the pre-stretch would change the deformation contour shape from a pyramid (which is typically seen in fabrics with no pre-stretch) into a cone [87].

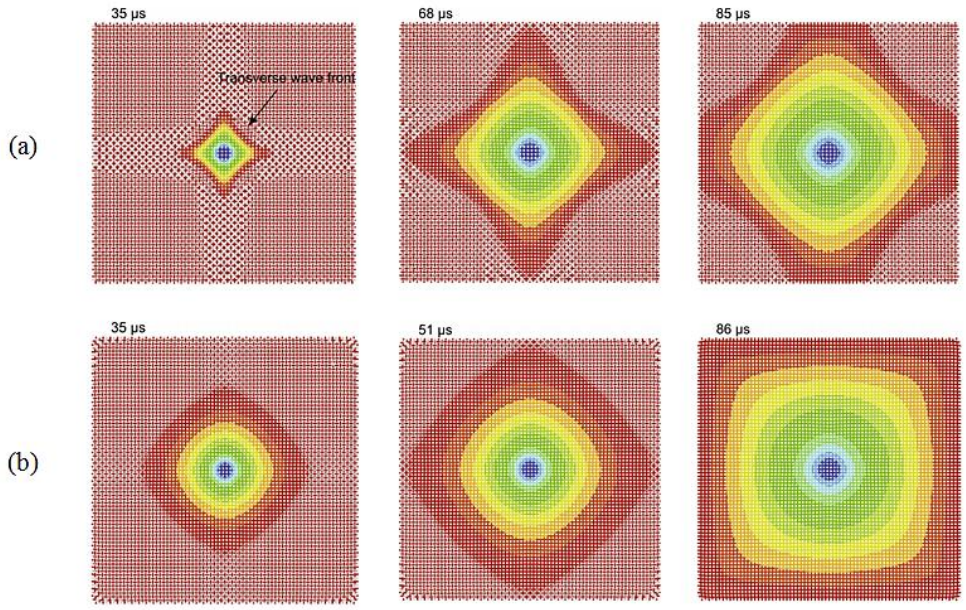

Fig. 7 (a) Deflection contours of model without pre-stretched at three different time (b) Deflection contours of 0.8% pre-stretched model at three different time [87]. Reprinted with permission from ref. 87 (Copyright © 2018 Elsevier).

2.3.6. Boundary condition

Woven fabric impact responses are strongly influenced by the boundary conditions [88]. Gürgen et al. [89] numerically modeled and evaluated the dependence of woven fabric ballistic behavior on boundary conditions. They utilized fully-fixed and two-fixed/two-free edges as the boundary conditions. The latter was reported to lead to projectile deceleration in an extended time under a low velocity impact. However, the difference between the two boundary conditions was smaller at larger impact velocities. Likewise, Duan et al. [90] studied four edges clamped, two opposite edges clamped, and four fabric edges left free boundary conditions by the finite element method (FEM). They modeled transverse impacts on plain-woven Kevlar fabrics with a single layer. The four edges left free boundary condition was found to decelerate the projectile effectively. Also, the four-edges-clamped boundary condition resulted in the largest projectile deceleration rate, as shown in Fig. 8(i). According to Fig. 8(ii), under the four-edges-left-free boundary condition, the impact broke a small number of yarns. As the impact

zone experienced a local fracture, the projectile deceleration ability of the fabric declines at later impact phases under the two- or four-edges-clamped boundary condition.

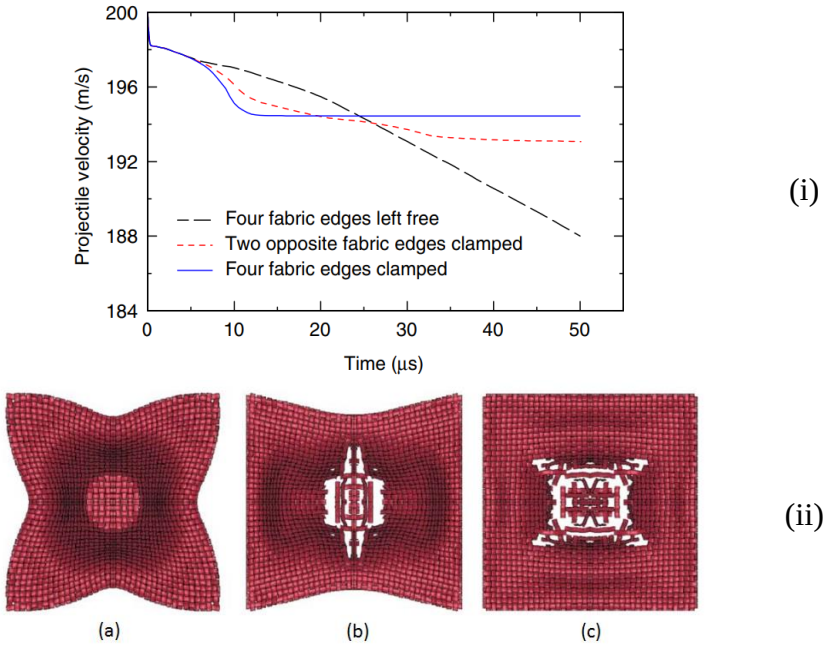

Fig. 8 (i) The projectile velocity as a function of time withinitial velocity of 200 m/s for different boundary conditions of fabric (ii) The fabric deformation at 40 μs with different boundary conditions under projectile impact with initial velocity of 200 m/s (a) Four fabric edges left free. (b) Two opposite fabric edges clamped. (c) Four fabric edges clamped[90].Reprinted with permission from ref. 90 (Copyright © 2006 Elsevier).

3. Standards of evaluation of soft composites as protective armor

Several body armor performance evaluation standards have been introduced, such as National Institute of Justice (NIJ), USA: NIJ 0101.06, NATO STANAG 4569, Home Office Scientific Development Branch (UK), GOST Ballistic Standards (Russia), European Ballistic Standards (EU), International Ballistic Standards, and German SCHUTZKLASSE standard [53]. STANAG 2920 (NATO Standardization Agreement) and MIL-STD-662F (Military Standard) are common fragment standards. Researchers most often apply NIJ 0101.06 to evaluate body armors. Furthermore, the NIJ (National Institute of Justice, USA) standard is adopted to measure body armor impact resistance

for gunfire torso protection purposes. Such standards require stopping ballistic-impact projectiles [1].

Blunt trauma or back face signature (BFS) is a crucial soft armor assessment aspect. It is often examined under non-perforation impacts. The backing material of armors undergoes a crater or trauma with a specific volume, depth, or diameter while stopping projectiles which indicates energy transmission to the backsides of the armors. Thus, it is required to measure the post-ballistic test volume, depth, and diameter of the trauma. The NIJ standard allows for a maximum BFS of 44 mm. A depth of penetration above 44 mm would cause the wearer serious blunt trauma. The trauma is measured by backing or supporting the test panel through a substance of high deformability. For volumetric and linear post-test measurements, clay backing is a good candidate. As a result, clay backing is widely employed to evaluate blunt trauma [17].

The armor ballistic performance evaluation setup involves a clamping material, a stand-mounted weapon, and two chronographs. The chronographs measure the velocity of the projectile. The projectile passes through the first chronograph, placed in front ofthe target, and thereafter through the second chronograph, placed just behind the target. Impact energy absorption represents the kinetic energy loss of the projectile in the perforation zone. To calculate the impact energy absorption, the initial and residual velocities are employed as [77, 91]:

$$\text{Initial energy of projectile before impact (J)} = \frac{1}{2} m_P V_i^{\,2} \quad (1)$$

$$\text{Residual energy of projectile after impact (J)} = \frac{1}{2} m_P V_r^{\,2} \quad (2)$$

$$\text{Energy absorbed by target (J)} = \frac{1}{2} m_P \left(V_i^{\,2} - V_r^{\,2}\right) \quad (3)$$

Where m_P (kg) is mass of projectile, V_i (m/s) is projectile initial velocity and V_r (m/s) is residual velocity.

4.Enhancement of impact performance of fabric

As a category of composites, polymer matrix composites are fabricated by applying polymer-based matrix reinforcement to fabrics. The use of different reinforcement matrixes in woven fabrics provides different composites in terms of ballistic performance. Such composites are still under the dominance of thermoset (TS) matrixes since they remain unchanged in stiffness under temperature variations and are suitable for fabric impregnation. A large number of works analyzed the impact behavior and energy absorption of TS matrix composites[92-95]. Despite the favorable mechanical properties of TS resin, this resin yields inflexible, hard composites, reducing the ballistic performance of fabrics [96]. Hence, researchers began to study other polymer matrixes.

Impact resistance is enhanced by the inter-yarn friction of woven fabrics. A number of frictional fabric enhancement techniques have been developed[97]. Plasma modification and chemical deposition can be employed in surface treatment and friction enhancement [98, 99]. However, these techniques involve heating and may lead to physical degradation. Moreover, fabric ballistic performance may be improved using adhesive spray coating [100]. Furthermore Coating fabrics with particle additives reinforced polymer is a promising method to increase friction and impact response of fabric [101, 102].

Shear thickening fluid (STF) impregnation is the most common method to increase the inter-yarn friction. STF is a non-Newtonian fluid with liquid-like behavior in the absence of loads, and the application of a large shear rate makes it a stiff solid[103]. In impregnated fabrics, a major STF responsibility is enhancing inter-fiber fiction under an impact load. Such inter-yarn friction interaction enhances the ballistic characteristics of fabric/STF composites. Rubber coating is also an innovative method

of impact resistance enhancement for woven fabrics. Natural rubber (NR) is employed as a suitable material for numerous purposes since it has great damping properties, significant puncture resistance, large flexibility, and desirable fabric adhesion. Hence, researchers have exploited NR for coating, shock absorption, and impact resistance panels in numerous textile applications. STFs and NR matrixes which enhance woven fabric ballistic performance via fabric flexibility preservation, are discussed in detail below. In addition, fabric-STF and fabric-rubber composites are evaluated in terms of impact resistance.

5. Fabric/STF composite

This section discusses the shear thickening mechanism and the factors that affect the shear thickening. Furthermore, fabric-STF composites are evaluated in terms of stab and high velocity impact resistance experimentally and numerically. Eventually the role of shear thickening fluid in energy absorption of fabric/STF composite.

5.1. Shear thickening fluid

In general, one can classify fluids into two main groups based on viscosity behavior under shear, including Newtonian fluids and non-Newtonian fluids. A Newtonian fluid has fixed viscosity under shear variations. A non-Newtonian fluid, on the other hand, exhibits a non-constant viscosity under shear rate elevation. Shear thickening fluid (STF) is one of the non-Newtonian fluids, and its viscosity rises due to increased shear rate [104]. Shear thickening happens in concentrated hard-solid-particle-containing colloidal suspensions. At the beginning of shear, STF exhibits shear thinning. The main characteristic of an STF, however, is an expected viscosity rise at a critical level of

shear rate. At the critical shear rate, a liquid-like material convertsinto a solid-like one. Fig. 9 illustrates the phenomenon of shear thickening [91].

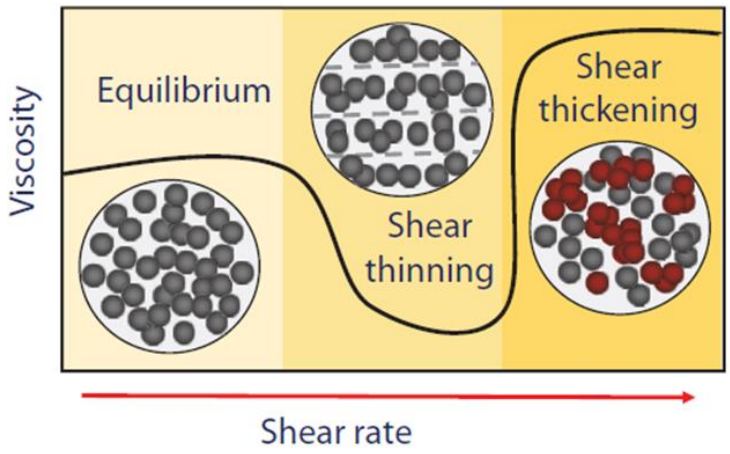

Fig 9. Schematic representation of shear thickening behavior [91]. Reprinted with permission from ref. 91 (Copyright © 2018 Wiley).

Today, shear thickening is of high interest to researchers. It used to be considered as a drawback as it limited the speed of industrial processes that had great shear rates and suspensions with large concentrations [105]. However, shear thickening has recently been exploited to develop smart composites. Protective applications appear as a major field of interest for STFs. Pioneer works, e.g., Wagner et al. [106], demonstrated that STF provided enhancement in protective systems. Later, a large number of works were conducted on the efficiency enhancement of protective systems, e.g., STFs and fabrics.

5.2. Shear thickening mechanism

A number of theories have been introduced for the purpose of explaining the mechanism of shear thickening, including the contact rheology, hydroclusters, and order-disorder transition mechanisms. Order-disorder transition was introduced by Hoffman [107, 108] as the earliest shear-thickening mechanism. Hoffman proposed that

particles are of ordered packing at initial small shear rates on account of intrinsic inter-particle repulsive interaction within a solution, which is preventive of their accumulation. A rise in the shear rate above the critical value pulls the particles out of the ordered configuration, makes them concentrate onto each other, and rapidly raises the viscosity, leading to shear thickening. The formation of a self-organized non-balanced bound microstructure, which is referred to as clusters, was the second earliest shear-thickening mechanism proposed [109, 110]. At a small shear rate, inter-particle interactions, whether Brownian or electrostatic, provide easy flow in the suspension. Clusters form at the critical shear rate at which hydrodynamic forces dominate the repulsive forces between particles, compacting particles in the form of dense squads and enhancing viscosity. A number of works were supportive of hydro-cluster shear-thickening theory by rheological examinations and numerical simulations[109, 111, 112].

Some studies recently introduced the contact rheology model [113, 114]. Denn et al. [114] argued hydro-clustering to dominate suspensions at small shear rates on account of non-contact rheology; however, they suggested that contact forces are of high effectiveness at the jamming point at which particles meet each other at large shear rates. A rise above the critical shear rate makes the contact forces form thickening-dominating lattices with inadequate hydrodynamic interaction. The loading of SiO_2 nanoparticles is of high importance in contact rheology as a rise in the suspension particle concentration raises the likelihood of a contracted microstructure[115].

5.3. Parameters influence the shear thickening

A number of factors, including the additive substance, particle shape, particle size, particle roughness, particle hardness, particle modification and particle volume fraction influence STF properties. These parameters are reviewed in this section.

STFs are involve a liquid phase and a solid phase which is observed in a wide range of suspensions[116]. Single-phase STF studies have mostly been focused on the utilization of SiO_2 particles as the solid phase[117].Unlike single-phase STFs, the influence of adding substances to STFs has been subject to a small number of studies[118, 119]. Multi-phase STFs are mixtures of single-phase STFs and various kinds of additives such asceramic particles[120], metal particles [121], Graphene oxide (GO)[122],Graphenenanoplatelet[123], CaCO3 particles[124] and Carbon nanotubes (CNTs)[125-127]. Such novel fluids allow for developing multi-functional composites that help tune the rheological properties with respect to the application field.Gürgen et al. [128, 129] explored the influences of multi-phase STFs on fabrics in terms of ballistic performance. SiC particles were studied as the secondary STF phase [130, 131]. Fig. 10 compares the neat and single- and multi-phase STF-impregnated targets under knife and spike impacts in terms of stab resistance [130]. They employed the SiC particle sizes of1.114, 0.512, and 0.340 μm, which were referred to as SiC-A, SiC-B, and SiC-C, respectively. The penetration depth increased as the energy of the impact rose. The neat target had lower stab resistance than the impregnated ones. Thus, single- and multi-phase STF treatment substantially enhanced fabric stab resistance, particularly under spike impacts.

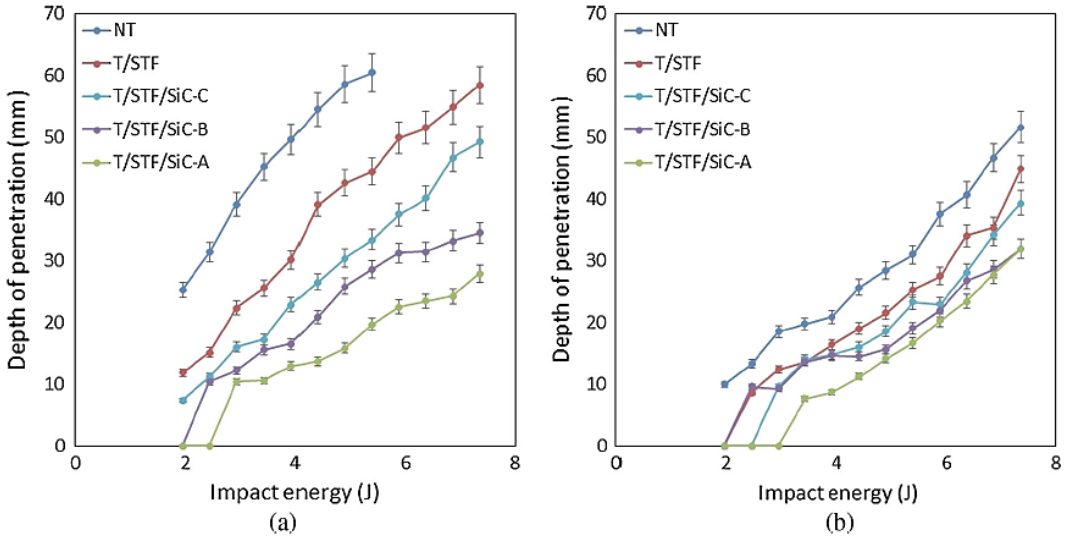

Fig. 10 Depth of penetration for (a) the spike and (b) the knife impactor[130]. Reprinted with permission from ref. 130 (Copyright © 2017 Elsevier).

The particle size is another important factor that influences the rheological performance of STFs. The critical shear rate was demonstrated to roughly decline due to a rise in the size of particles[132]. Flow curves undergo a systematic shift to smaller shear stresses as the particle size increases. This may be partially accounted for via shear stress scaling through the Brownian stress [133]. Furthermore, a rise in the particle size increased the viscosityand shear thinning degree before shear-thickening occurred [134].

The shape of particles significantly affects the rheological behavior of a concentrated colloidal suspension[53]. Wei et al. [135] fabricated STFs with two particle shapes including irregular and spherical SiO_2 nanoparticles to explore the influences of the particle shape on SiO_2-based STF properties. Fig. 11 depicts the rheological STF properties. According to Fig. 11a, the spherical SiO_2-STF had a critical shear rate of nearly 14.13 s^{-1}, and its viscosity rose from 3.32 to 261.63 Pa.s (by approximately 78 times). Moreover, the irregular SiO_2-STF had a critical shear rate of nearly 1.65 s^{-1}, and its viscosity rose from 13.03 to 181.59 Pa.s (by approximately 14

times). According to Fig. 11b, the irregular SiO_2-STF had a slightly smaller initial viscosity than the spherical suspension, and no clear shear thinning was observed in the rheological examination.

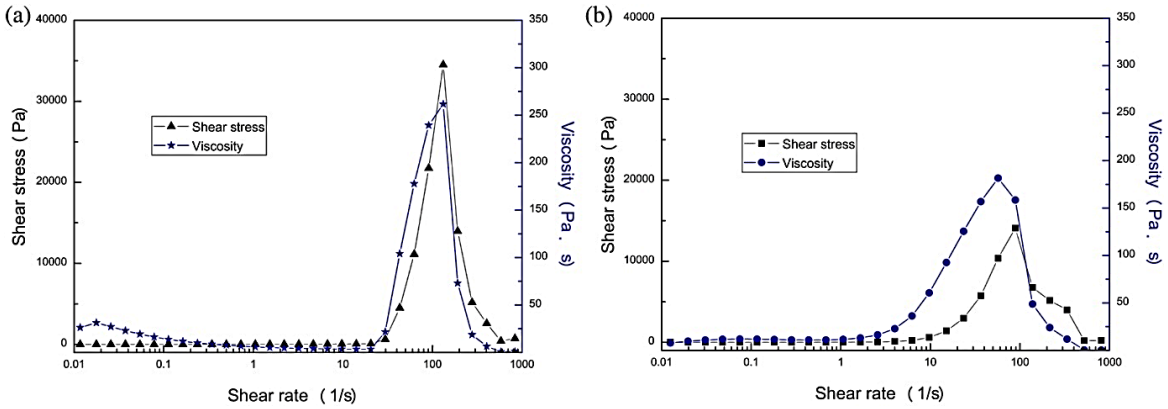

Fig. 11 Viscosity and shear stress versus shear rate (a) spherical silica-based STF; (b) irregular shapes silica-based STF [135]. Reprinted with permission from ref. 135 (Copyright © 2020 Wiley).

The modification of particles impacts rheological performance in STFs. Earlier works argued that it is possible to perform a modification procedure by using chemical or mechanical techniques[136, 137].It has been proved that heat treatment enhanced the shear thickening effect, particularly at a higher temperature. A rise in the temperature in heat treatment shifts the onset of shear thickening to smaller shear rates[138]. Li et al. [136] evaluated the contribution of acid treatment to STF rheological properties. It was found that the largest viscosity in shear thickening enhanced as HNO_3 rose to a certain concentration above which the viscosity began to decline, as illustrated in Fig. 12. As can be seen, a rise in the HNO_3 concentration reduces the critical shear rate for the onset of shear thickening. At an HNO_3 concentration above 8.50 $mol.L^{-1}$, a rise in the acid concentration raises the critical shear rate.

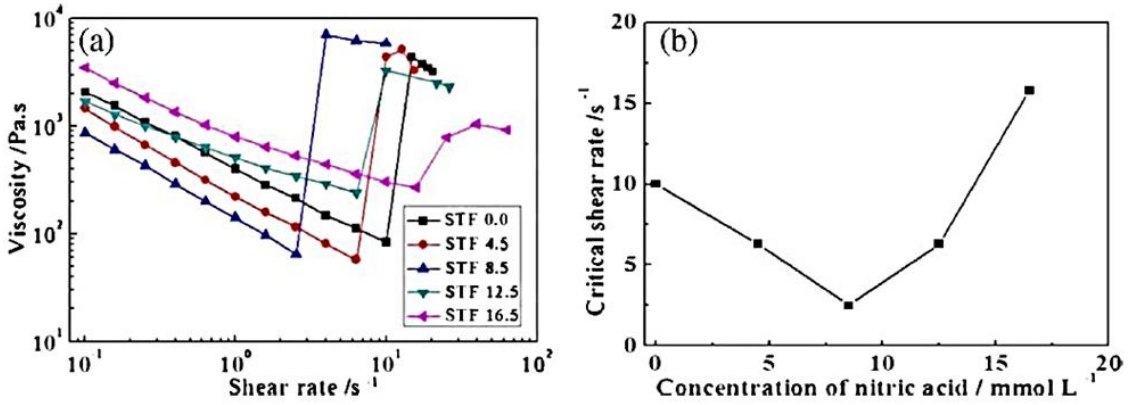

Fig. 12 The shear thickening behavior of suspensions with different HNO_3 concentration. (a) Viscosity as a function of shear rate. (b) Critical shear rate as a function of concentration of HNO_3 [136]. Reprinted with permission from ref. 136 (Copyright © 2016 Elsevier).

The roughness of particles influences the rheology of STFs. Earlier works compared spherical and fumed silica particles[132]. To fabricate fumed silica, a flame hydrolysis procedure is applied. The primary structure of fumed silica involves branch shapes, enhancing the roughness of the particle surface. Spherical silica particles, on the other hand, are smooth with slight surface asperity. fumed silica suspensions raise the mixture viscosity and decrease the critical shear rate [132]. The main reason in the viscosity increase is the increased surface area due to the complex geometry of the fumed silica.

The hardness of particles is another variable that impacts STF rheological behavior [139]. To evaluate the contributions of the hardness of particles, two nanoparticle types with different hardness degrees (i.e., polymethyl methacrylate and SiO_2) were employed for STF fabrication by Kalman et al. [140]. The STF with harder particles were demonstrated to have a larger critical shear rate and critical shear stress. Harder particles have a higher capability of resisting stress elevation and thus bearing larger stresses at large shear rates.

The particle concentration is another parameter that substantially impacts STF rheological performance. All STFs with different concentrations of particles exhibit

both shear thickening behavior and shear thinning behavior. Shear-thinning and thickening occur at small and large shear rates, respectively[77, 141]. According to Fig. 13, a rise in the weight fraction of particles increased the viscosity plot of an STF. A rise in the concentration of nanoparticles reduces the inter-particle distances and leads to a higher number of large-sized hydroclusters at a small shear rate. This significantly increases shear thickening behavior. An increase in the nanoparticle fraction induces greater shear thickening behavior and a sharper viscosity enhancement at a smaller critical shear rate [142, 143]. A rise in the volume fraction of nanoparticles enhances the hydrodynamic forces in light of inter-particle distance reduction, and repulsive forces could be handled at a smaller shear rate.

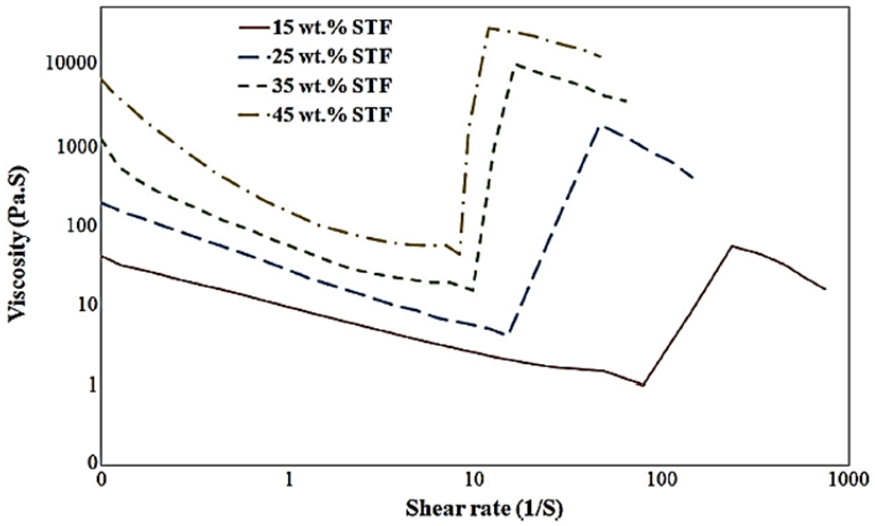

Fig. 13 Rheological behavior of PEG/Silica STF [77]. Reprinted with permission from ref. 77 (Copyright © 2019 Elsevier).

5.4. Quasi-static test of fabric/STF composite

5.4.1. Preparation of fabric/STF composite

The high-performance fabric treatment of STFs has been of great interest concerning body protection. Studies mostly reported substantially-improved fabric impact resistance through STFs. Impregnation has typically been exploited for the fabrication of fabric/STF composites. To add STF in fabric impregnation, a proper medium was employed to mix nanoparticles at the required fractions. Mixing was performed using ultrasonic, mechanical, or magnetic devices. High suspension viscosity makes the uniform impregnation of fabrics difficult. Thus, alcohols are employed to dilute suspensions for the easier STF impregnation of fabrics. Then, the fabric undergoes soaking in the diluted suspension, with the diluted STF penetrating the inter-yarn spaces via padding, prior to the alcohol removal of the fabric within a convection oven [131, 144].

5.4.2. Yarn pull-out test from fabric/STF composite

Fiber friction enhancement has been found to be a major contribution of STFs to impregnated fabrics [145, 146]. It is possible to estimate the inter-yarn friction by pullout tests [147]. Thus, the STF impregnation of fabrics raises the pullout force of yarns on account of enhanced friction between the yarns[131, 148-150]. The yarn pullout force arises from the warp-weft friction accumulation at the interlacing point. It involves static and sliding friction [151]. At the beginning of the pullout testing of yarns, the crimping yarns undergo top-to-bottom straightening as the static friction and pullout force rise until the peak. Once the pullout force exceeds the static friction threshold, it reduces and fluctuates while the free yarn end passes the crossing yarns. Each fluctuation represents a local graph peak arising from the stick-slip motion in the

pullout process. Eventually, the pulled yarn removal of the fabric is completed. In the static friction phase, the ultimate pullout force of the neat fabric happened. In contrast, the maximum impregnated fabric pullout force occurs in the dynamic friction phase [149].

The addition of SiO_2 nanoparticles in an STF was demonstrated to change the friction between the yarns. This leads to a larger pullout load [152]. For example, Khodadadi et al. [77] subjected fabrics impregnated with STF to pullout tests at the SiO_2 weight fractions of 15%, 25%, 35%, and 45%. Fig. 14 depicts the pullout force versus the displacement for both the impregnated and neat fabrics. As can be seen, fabrics with STF impregnation had larger frictional loads. This stems from the nanoparticles positioned in the inter-fiber spaces, interlocking the fibers. Thus, a rise in the nanoparticle fraction increases the required pullout load for overcoming the friction between fabric yarns. The pullout curve suggests that a significantly greater gradual reduction occurred in the load above the peak. As another finding in the pullout test, the fabric with STF impregnation had a stiffer response (i.e., a steep initial increase) than the neat fabric [77].

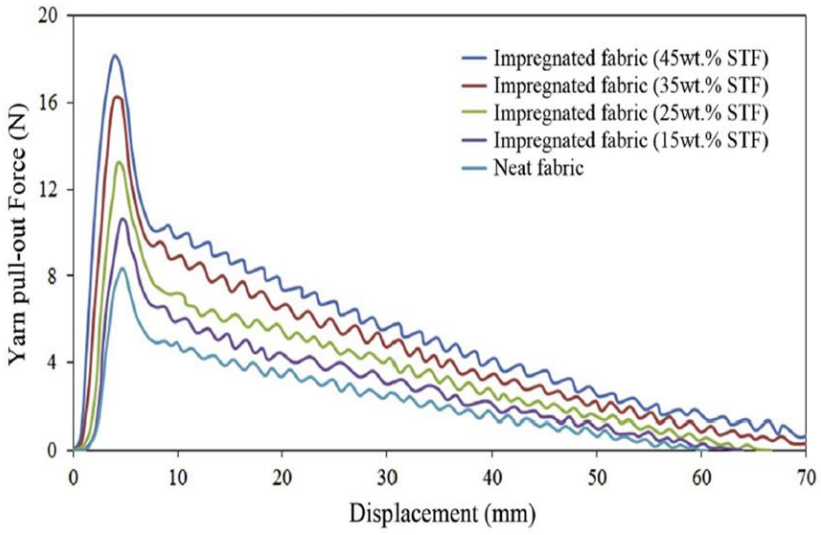

Fig. 14 Yarn pull-out force versus displacement curve [77]. Reprinted with permission from ref. 77 (Copyright © 2019 Elsevier).

Additionally, SiO_2 microspheres with higher hardness can be incorporated into softer filaments to obtain stronger direct filament-yarn coupling [140]. Bajya et al. [148]employed SiO_2 nanoparticles with sizes of 100 and 500 nm to fabricate impregnated fabrics. The peak yarn pullout load was demonstrated to be greater at a smaller nanoparticle size since the fabric with smaller nanoparticles had a larger specific surface area and more nanoparticles in the STF. Thus, it more properly coats the surface of filaments, leading to a larger pullout load of yarns. In contrast, Mawkhlieng[153] observed that STF treatment with different sizes of SiO_2 nanoparticles did not exhibit a significant difference in the peak force within the Kevlar fabric.

5.4.3. Stab resistance of fabric/STF composite

A rise in the inter-yarn pullout load yields additional energy dissipation, thereby enhancing STF/fabric composites in the absorption of energy [154]. This suggests that a higher pullout force of yarns leads to a higher ability to resist impacts and contributes to the absorption of energy by extending fiber rupture. In low-velocity and quasi-static settings, studies mostly reported substantially-improved textile fabric energy absorption through STFs[155-157]. Generally, one can divide stab resistance into two groups: knife stab and puncture resistance. Stab resistance refers to resisting the penetration of sharp-edged knives or sharp-tipped objects. Gong et al. [156] evaluated the influence of STF components on resistance to knife stab and puncture in STF-reinforced fabrics. They demonstrated that STF particle hardness dominated the STF-reinforced fabrics in knife stab resistance. However, the friction between yarns was found to determine puncture resistance. Qin et al. [151] argued mechanical properties and stab resistance in the Kevlar fabric to be strongly improved by the optimal STF content. A rise in the STF

content raised the resistance of STF-reinforced Kevlar fabric (STKF) to stab. Also, the optimal stab resistance occurred at an SFT weight fraction of 34.89%. Gürgen et al. [128]performed drop tower tests on STF-treated and neat fabrics in order to study composite systems in terms of stab resistance. They observed that the penetration depth of the STF-reinforced fabric was nearly three times lower than that of the neat specimen. Xu et al. [158]explored the impacts of the size and weight fraction of SiO_2 nanoparticles on STF-reinforced woven-fabric panels. STFs were fabricated by using SiO_2 nanoparticles with sizes of 12 and 650 nm. Three weight fractions were applied under each nanoparticle size. Figs. 15a and 15b demonstrate the peak load and total absorption of energy, respectively. At both nanoparticle sizes, a rise in the weight fraction clearly raised the peak impact load and total absorption of energy. Li et al. [159]verified that STF is helpful in enhancing UHMWPE fabrics in stab resistance by reducing the mobility of yarns as well as fabric transverse response acceleration.

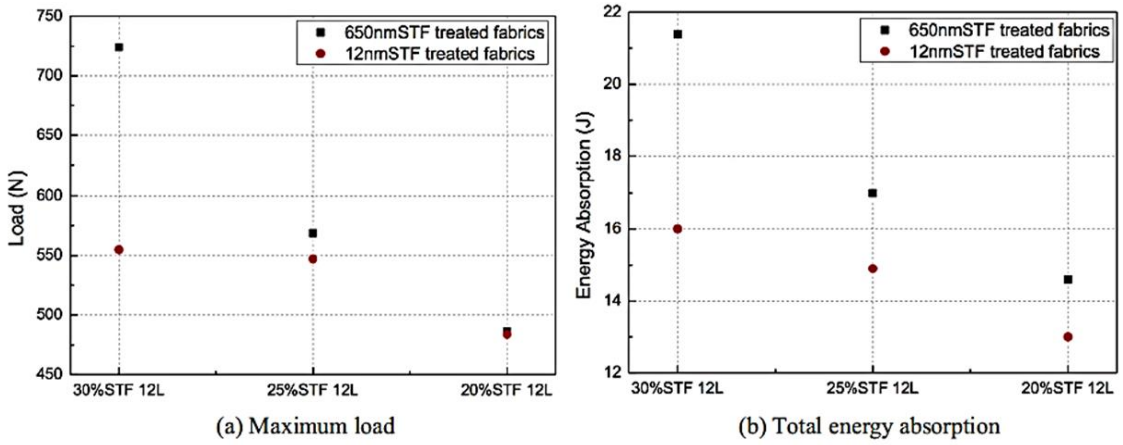

Fig. 15 Nanoparticle size and weight fraction effect on panel performance [158]. Reprinted with permission from ref. 158 (Copyright © 2017 Elsevier).

Li et al. [159] studied the dynamic stab resistance characteristics of STF-impregnated UHMWPE fabrics. Fiber fracture was demonstrated to occur in both STF-impregnated and neat fabrics after a number of yarns were pulled out of the fabric after

the knife stab test of the neat fabric, as shown in Fig. 16. An STF-impregnated UHMWPE fabric undergoes lower damage and deformation than a neat fabric.

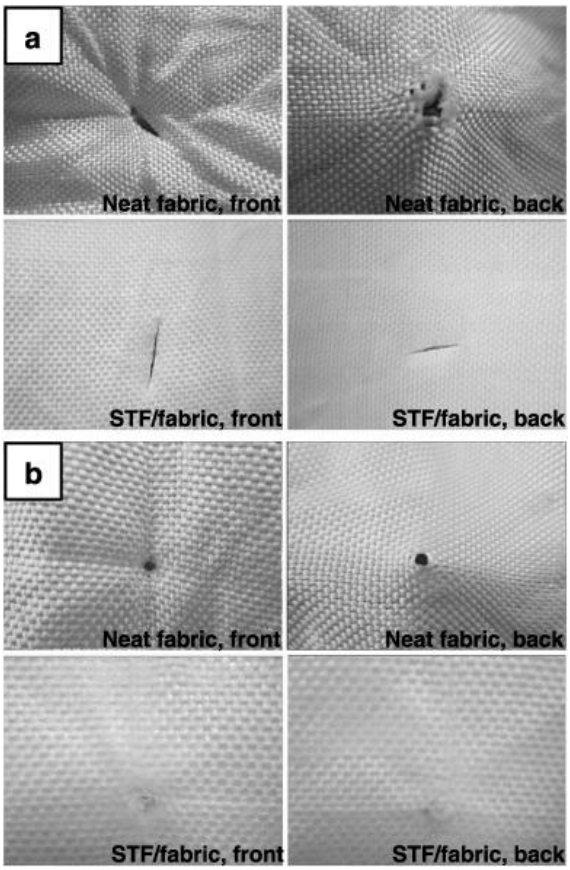

Fig. 16 Dynamic stab test of neat UHMWPE specimen and STF/UHMWPE specimen (a) by knife impactor and (b) spike impactor[159]. Reprinted with permission from ref. 159 (Copyright © 2016 Elsevier).

5.5. Impact response of fabric/STF composite

At a high velocity, previous studies employed a gas gun to subject fabric/STF composites to ballistic tests[131, 147, 160-164]. A number of studies reported aramid-based armors to have higher ballistic impact resistance after STF treatment[160, 165]. Tan et al.[166]studied SiO_2 colloidal water suspension (SWS)-impregnated aramid-based fabrics in terms of ballistic behavior at various concentrations of nanoparticles in water. Single-, two-, four-, and six-ply SWS-impregnated fabrics with the weight fractions of 0%, 20%, 40%, and 50% underwent comparisons to an untreated neat fabric

in terms of specific ballistic energy and ballistic limits. The ballistic limits of the two-ply fabric with an SWS weight fraction of 40% were found to be 70% greater than that of the neat two-ply fabric. Ballistic resistance improvement was believed to arise from enhanced friction between the fabric and projectile and increased friction between the yarns due to the SiO_2 nanoparticles and clusters. The STF impregnation-induced enhancement in frictional characteristics restricted yarn motion and encouraged the adjacent yarns for projectile arrestment. An STF-reinforced fabric can preserve weave integration under an impact[167, 168]. Local STF-impregnated fabric structures are properly preserved in the impact area, whereas a neat fabric structure undergoes substantial distortion under an impact.

It is worth noting that fabric layers have small actual breakage of fibers, despite the possible occurrence of stretching in the vicinity of the impact location. In contrast, impregnated fabrics exhibit large breakage of fibers in the vicinity of the projectile contact location, and very small pullout or wrinkling of yarns around the fabric [168]. The pullout of fibers is of higher distinction, with the fiber pullout-induced horizontal and vertical patterns during neat Kevlar penetration. However, STF-reinforced Kevlar fabrics exhibited lower pullout development. Fig. 17 depicts the fabric pattern and the formation of pullout fibers on both front and rear penetration hole sides. As can be seen, the STF-reinforced Kevlar fabrics exhibited larger deformation localization than the neat fabric.

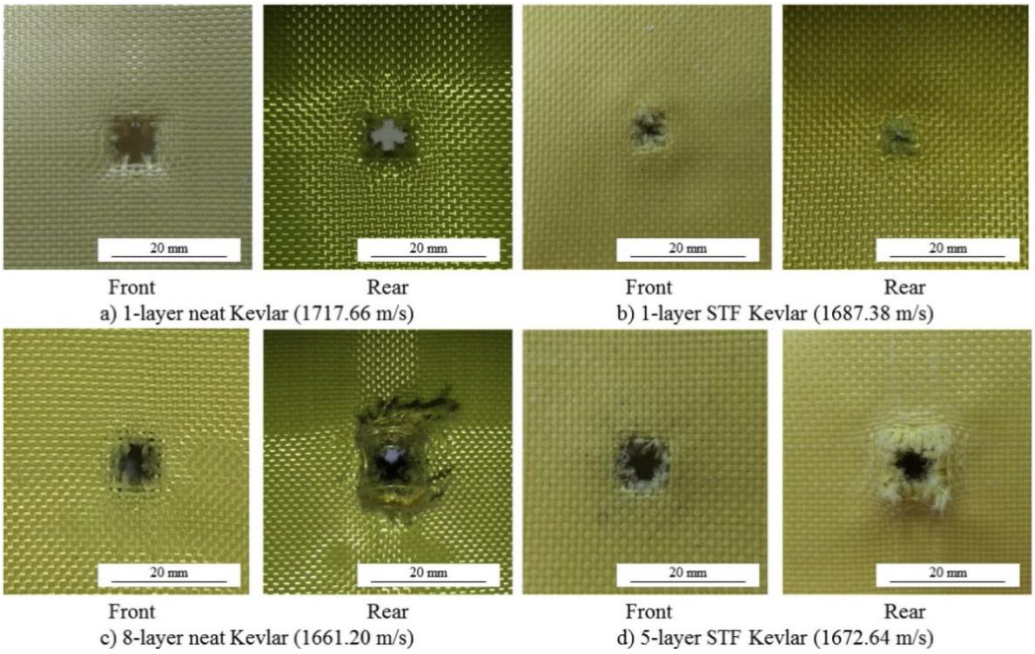

Fig. 17 Front and rear perforation of neat and impregnated specimens [160]. Reprinted with permission from ref. 160 (Copyright © 2014 Elsevier).

It is worth mentioning that the STF effect is dependent on a number of variables, including the fabric structure, Panel configuration, angular orientations and thread density [169-172]. Laha and Majumdar[173]fabricated five weave patterns by changing the paramid (Technora) yarn density and incorporated treatment using an STF suspension at a fraction of 60% to produce soft armor materials. It was observed that infirm weave patterns enjoyed higher impact energy absorption improvement, and untreated infirm weaves exhibited low impact resistance. It was also found that a rise in the density of threads in a specific weave decreased the impact energy absorption improvement. Likewise, Arora [174] suggested that STF treatment in firm structures with greater fabric sett reduces impact resistance on account of stress concentration. An infirm fabric with the same yarns and smaller sett, however, exhibited impact resistance improvement after treatment by an STF.

5.6. Numerical simulation of impact on fabric/STF composite

A large number of empirical studies were conducted on fabric/STF composites under ballistic impacts. However, few numerical studies investigated such composites [175].

Numerical fabric/STF composite studies mostly assumed friction to be the main factor in such composites for their impact resistance, irrespective of the shear thickening effect [161, 167, 176-178]. Hasanzadeh[177] studied STF-reinforced high-modulus polypropylene (HMPP) and neat fabrics in terms of ballistic behavior under high-velocity impacts. Also, they numerically evaluated backside deformation and back face signature on the clay witness. In order to obtain the mechanical properties of the STF-treated and neat fabrics, pullout and tensile tests were carried out on the fabrics. The STF impregnation contribution was studied in the form of inter-yarn friction, yarn crossover, and fabric-projectile friction during an impact. Gürgen[178] proposed a numerical technique to model the impact performance of multi-phase STF-reinforced projective fabrics. The main contribution of the STF was proposed to be the frictional enhancement, based on the inter-yarn and surface friction tests. In this sense, neat, single-phase, and multi-phase STF-reinforced fabrics were subjected to frictional tests. The test results were exploited to construct a numerical model for the impact performance simulation of fabrics under various treatments. Fig. 18 demonstrates the experimental and numerical local deformations of the untreated and treated fabrics. The experimental and numerical results were found to be consistent, suggesting that it is rational and possible to apply a friction-based technique to fabric ballistic resistance.

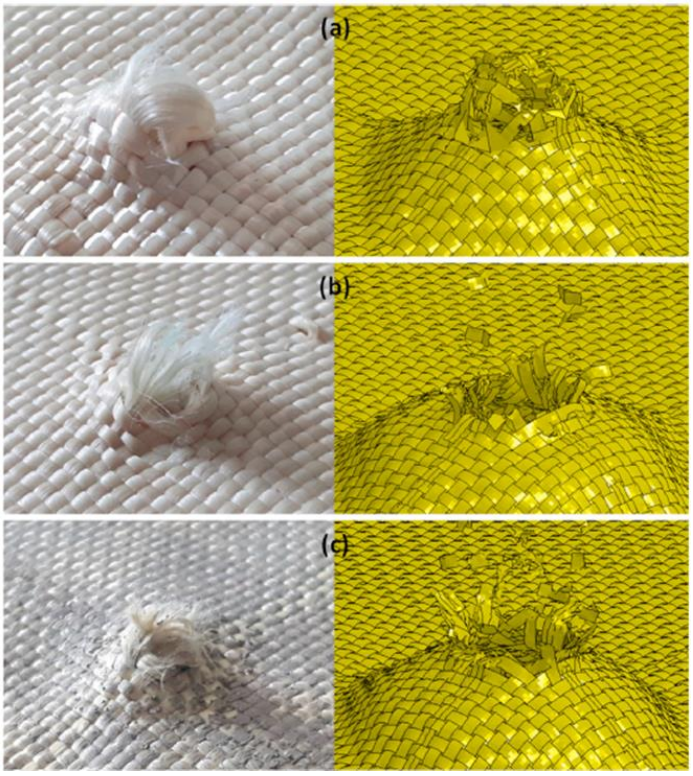

Fig. 18 Experimental and numerical results of impact on (a) NT, (b) S-STF and (c) M-STF [178]. Reprinted with permission from ref. 178 (Copyright © 2020 Elsevier).

Additionally, the fluid-solid coupling analysis is employed to model STFs. In such an analysis, an STF is considered to be a viscous fluid by an Euler grid. A comprehensive STF-reinforced fabric model was developed by Rabb et al.[179]. The model could represent the viscous, frictional, and thermodynamic effects. The hybrid-particle-element (HPE) technique was modified by a generalized Bingham fluid model and an equation of state (EOS) to incorporate STF effects. Yarn-level fabric modeling was performed, and a mixture equation of state was introduced for fabric particles to represent the STF thermodynamic effects.

Lu et al. [180] employed the microstructural finite element method (FEM) to study the impact performance of STF-impregnated warp-knitted space fabrics (WKSFs) subjected to impacts. To incorporate three characteristic regions of the general curve of STF viscosity (i.e., shear-thinning, Newtonian region, and shear-thickening), they defined a shear thickening viscosity function as:

$$|\eta(\dot{\gamma})| = \begin{cases} m_I \dot{\gamma}^{n_I - 1} & \text{for } \eta_c \leq \eta \leq \eta_0 \\ m_{II} \dot{\gamma}^{n_{II} - 1} & \text{for } \eta_c \leq \eta \leq \eta_{max} \\ m_{III} \dot{\gamma}^{n_{III} - 1} & \text{for } \eta_e \leq \eta \leq \eta_{max} \end{cases} \quad (2)$$

In which η is the apparent viscosity, $\dot{\gamma}$ is the shear rate, m is the flow consistency index, and n is the flow behavior index. In the model, the STF was fabricated as an Eulerian part. Also, Eulerian analysis was employed in the FEA model. They demonstrated the STF behavior and yarn-fluid interaction to play a key role in the impact energy absorption and impact deformation mechanisms. Sen et al. [181] adopted the coupled Eulerian-Lagrangian (CEL) approach to investigate composite ballistic responses. In this approach, they modeled Kevlar yarns by the Lagrangian membrane elements and incorporated the STF into an Eulerian mesh. A CEL model was constructed in ABAQUS for an STF-Kevlar fabric. Fig. 19 shows the projectile system. A contact algorithm was utilized to establish STF-Kevlar interaction. At up to the critical strain, Kevlar is considered as a linear elastic material. However, Kevlar shows brittle failure above the critical strain. Rate-dependent viscosity and EOS characterize an STF.

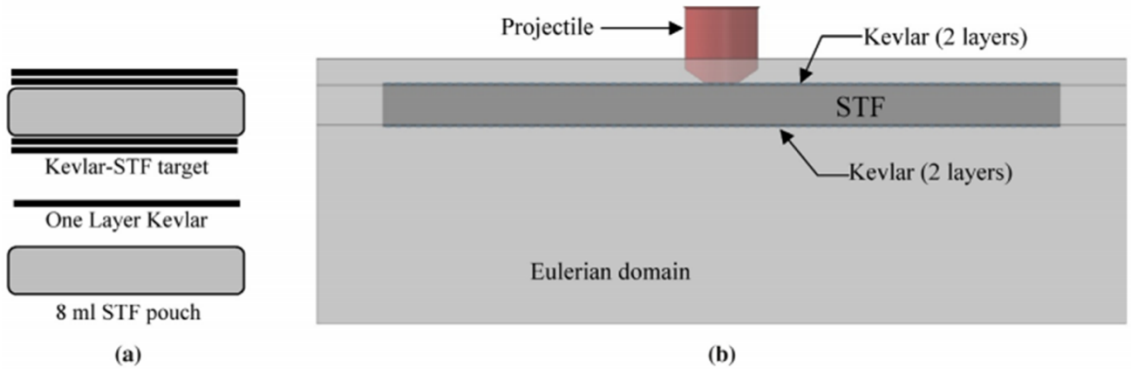

Fig. 19 (a) Kevlar-STF layered composite target (b) Numerical model of Kevlar-STF layered composite under projectile impact loading [181]. Reprinted with permission from ref. 181 (Copyright © 2019 Elsevier).

5.7. Role of shear thickening fluid in energy absorption of fabric/STF composite

Studies argued the absorption of energy by a fabric/STF composite to be heavily dependent on the friction between the yarns rather than STF rheology[117, 182, 183]. As mentioned, the pullout results demonstrated the friction between yarns to be the most prominent factor in fabric impact resistance. However, a number of studies are not supportive of the claim that friction is the main energy absorption mechanism of impregnated fabrics. Mawkhlieng et al. [153] evaluated STF contributions to the impact resistance improvement of high-performance fabrics. They employed mono- and bi-dispersed SiO_2 nanoparticles to fabricate STFs. The rheological findings revealed that the mono-dispersed SiO_2 STFs exhibited discontinuous shear thickening behavior and larger peak viscosity. As a yarn-to-yarn friction measure, the pullout force of yarns demonstrated no significant difference between STF-treated fabrics. Furthermore, impacts tests at low velocities indicated improved energy absorption for mono-dispersed SiO_2-treated fabrics. Eventually, it was proposed thatSTF rheological behavior makes a substantial contribution to the enhancement of impact resistance [153]. Liu et al. [184]conducted another analysis of the effects of STFs on fabric impact resistance improvement. They fabricated two series of STFs by using spherical SiO_2 nanoparticles with the diameters of 100 and 650 nm at various concentrations. The critical shear rate was 0.6-3.2 and 169-627 s^{-1}under the nanoparticle sizes of 650 and 100 nm, respectively. The findings of the impact tests revealed that the Kevlar fabric improved in impact resistance and energy absorption in light of the nanoparticles with a size of 100 nm. However, the nanoparticle size of 650 nm reduced STF treatment performance. They concluded that different suspension system trends arose from the specific shear rate with critical value.Since STF fills inter-yarn cavities of very small sizes and generate a non-continuous composition, solely very small STF drops exhibit shear

thickening at the impact location. This suggests that shear thickening could not be effectively beneficial to the fabrics [185].

5.8. Other applications of STFs

In light of specific characteristics of STFs, these materials may be employed for a variety of purposes, including medical products, sports products, mechanical platforms, space technologies, construction, automotive, mechanical dampers, and petrochemical applications [186]. Construction represents a potential context to employ STF-based sandwiches in order to improve building resistance under seismic and wind flutter impacts [187]. Also, in light of viscoelastic behavior, STFs can be beneficial in the isolation of structural vibration. Vibration damping may be enhanced using STF-based sandwiches [188]. Gürgen et al. [189]studied a sandwich structure in terms of vibration attenuation. The structure consisted of two aluminum face sheets surrounding an extruded polystyrene (XPS) foam core. A SiO2 nanoparticle-reinforced STF was employed to fill the core and modify the sheets. The incorporation of an STF into a sandwich structure was observed to substantially enhance vibration attenuation. Also, the use of STFs and SSPs in multi-layered cork structures in order to enhance vibration attenuation was studied. STFs and SPPs were found to improve cork layers in vibration attenuation [190]. The viscosity of pure STFs rises on account of shear thickening when subjected to impact loads. Also, a network of energy dissipation is created in the mixture by the particle contact-induced force chain. However, the energy absorption of composites is not adequately improved [185].

6. Fabric/NR composite

Composites have been of great interest in light of superb characteristics, including large strength, high stiffness, and high structural stability[191-193]. These characteristics have been subject to improvement efforts as composites suffer from a number of downsides, e.g., moisture sensitivity, residual stress, and small impact resistance[194]. Since the composite phase is brittle in nature, the incorporation of natural rubber (NR) was seemingly a rational approach. Strength and weight efficiency improvement has been considered in the literature, and rubbers have been employed for coating or laminate inter-layering in light of their capacity to absorb energy, despite the ongoing need for improving moisture seepage and delamination [195]. Enhancements in the impact performance of laminates containing elastomers could be primarily achieved by (1) high elastomer energy absorption, (2) material strain hardening, and (3) wider impact load distribution [196]. The following sections provide a brief discussion of the use of elastomers in laminated systems prior to the review of the elastomeric laminate literature.

6.1. Elastomers

The term “elastomer” deals with the terms “elastic” and “polymer.” Elastomers refer to a large group of amorphous polymers that can undergo significant elastic deformations with no fracture. Such materials not only enjoy a low glass transition temperature but also have high softness and low moduli of elasticity [197]. For these materials, the hysteretic damping capacity is essential in the control of vibrations and implementing acoustic insulation. Elastomeric molecules have high lengths and twisting and can undergo cross-linking by a curing agent. This process is referred to as vulcanization. Cross-linking raises the hardness of elastomers and makes the reshaping of the material impossible.

Synthetic and natural rubbers are two elastomer types that have been extensively employed for various purposes. The latter involves organic compound isoprene and small impurity contents of other organic materials along with water [195]. Due to its excessively large softness, it is modified in properties by the addition of filters, e.g., SiO_2, S, and carbon black [198]. It has satisfactory friction, fatigue, and abrasion resistance. However, the sunlight, heat, and oil resistance of natural rubber is low [197]. Synthetic rubber refers to any artificial rubber majorly derived from the by-products of petroleum [195]. Compared to natural rubber, synthetic rubber enjoys greater chemical, gasoline, and heat resistance, and has a wider temperature range of applicability. Synthetic rubber is mainly employed in the fabrication of belts, flooring, matting, and the automotive industry. Ethylene propylene, polybutadiene, styrene-butadiene, and butyl are among common synthetic rubber variants [197].

6.2. Impact response of fabric/NR composite

Elastomers have been extensively employed for engineering purposes [26, 199]. Fabric-reinforced rubber composites are turning out to be a proper alternative in ballistic and blast applications [200, 201] in light of significant damping characteristics [202] and flexibility [28]. A number of studies recently described and modeled the behavior of such composites[203-205].Heng et al. [206] proposed an anisotropic hyperviscoelastic constitutive model of reticulated fabric-reinforced rubber composites. They incorporated the influence of fibers, rubber-fabric interaction, temperature, and rubber viscoelastic characteristics.

A number of studies characterized the process of fabricating rubber composites. They evaluated the solution dipping technique for fabric coating via natural rubber (NR) by four approaches, i.e., single dip (SD), single dip-pad (SDP), double dip-pad-dip

(DPD), and double dip-dip (DD)[207]. They explored the effects of the coating approaches on the specimens in terms of ballistic performance. The SD-coated specimens were found to have larger absorption of energy, with a 28% higher ballistic limit than the neat specimen. Likewise, Hassim et al. [208] employed various dipping techniques to fabricate high-strength NR-coated UD fabrics. They utilized the SD, DD, and triple dip (TD) methods. The specimens were subjected to puncture resistance examination. The puncture loads of the TD-, DD-, and SD-coated specimens were found to be 62%, 47%, and 39% larger than that of the non-coated UD specimen, respectively.

Ahmad et al.[209, 210] studied the ballistic impact behavior of natural rubber latex (NRL)-coated fabrics. After NRL coating, the fabrics were integrated with non-coated specimens into various fabric configurations. Then, the fabrics underwent perforation for the evaluation of impact resistance. They integrated and stacked various fabric systems with eighteen and twenty-one layers, involving completely non-coated layers and a combination of non-coated and four coated layers. They found the entire NRL fabric configurations to have a smaller indention depth, irrespective of the layer count and configuration, as compared to the neat specimen. The puncture resistance results revealed that the fabrics with NRL coating exhibited a 21% larger puncture load than the non-coated ones [209]. Concerning NRL coating contributions to the pullout load of yarns, NRL coating generally raised the pullout load of yarns by 200% (for the warp specimens). It was found that coating enhanced the friction between fabric yarns [209].

Roy et al. [211] examined NR-coated fabrics in terms of ballistic behavior. They employed UHMWPE and Kevlar fabrics. It was observed that the NR coating of the UHMWPE and p-aramid fabrics increased the pullout load by 360% and 480%,

respectively. In comparison to the double-layered UHMWPE and Kevlar fabrics, the coated doubled layered UHMWPE and p-aramid fabrics experienced 81% and 44% rises in impact energy absorption, respectively. Fig. 20 compares the double-layered stitched NR-coated and uncoated p-aramid fabrics. Concerning the uncoated double-layered fabrics, the impacting object could pullout/break a number of primary yarns, leading to penetration. Concerning the coated fabrics, however, pullout/breakage did not occur. The enhanced NR-coated fabric layer bonding might have enhanced the coated p-aramid fabrics in impact behavior.

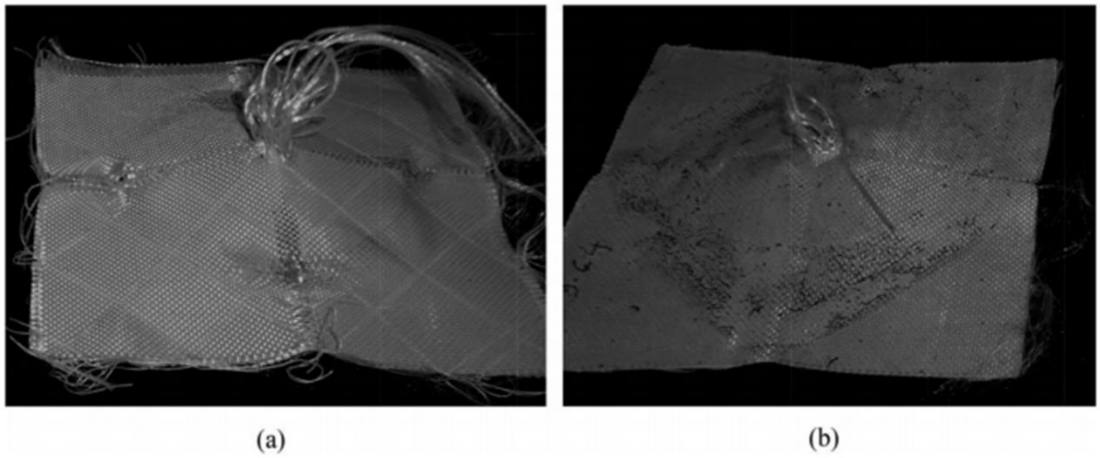

Fig. 20 Impact response of fabric (a) two layered stitched p-aramid fabric, (b) two layered NR coated p-aramid fabric [211]. Reprinted with permission from ref. 211 (Copyright © 2018 Wiley).

Roy et al. [212] compared Kevlar/epoxy composites to Kevlar/rubber ones in terms of energy absorption under impact loading with a high velocity. The elastomeric composite was observed to have a puncture load of 2.8 times as large as that of the stitched panels. Also, the Kevlar-epoxy composites were found to have a 6.6 times greater puncture load than stitched panels. Also, the elastomeric specimens exhibited 73% greater energy absorption than stitched panels. Furthermore, the Kevlar/epoxy composites exhibited a 86% decline [212].

Mahesh et al. [213-216] recently investigated flexible rubber composites. They evaluated the impact responses and mechanical properties of jute- and rubber-layered composites. In order to evaluate such flexible composites in terms of the low-velocity impact response, they applied various levels of impact energy to laminates in different stacking configurations, including jute/rubber/jute (JRJ), jute/rubber/rubber/jute (JRRJ), and jute/rubber/jute/rubber/jute (JRJRJ), by using a conical impacting object [215]. Fig. 21 depicts the peak flexible composite load variations under various impact energy levels. As can be seen, JRJRJ had the largest damage resistance among the stacking configurations. Also, they performed numerical, analytical, and experimental tests on the JRJ, JRRJ, and JRJRJ flexible laminates to evaluate their impact responses [216].

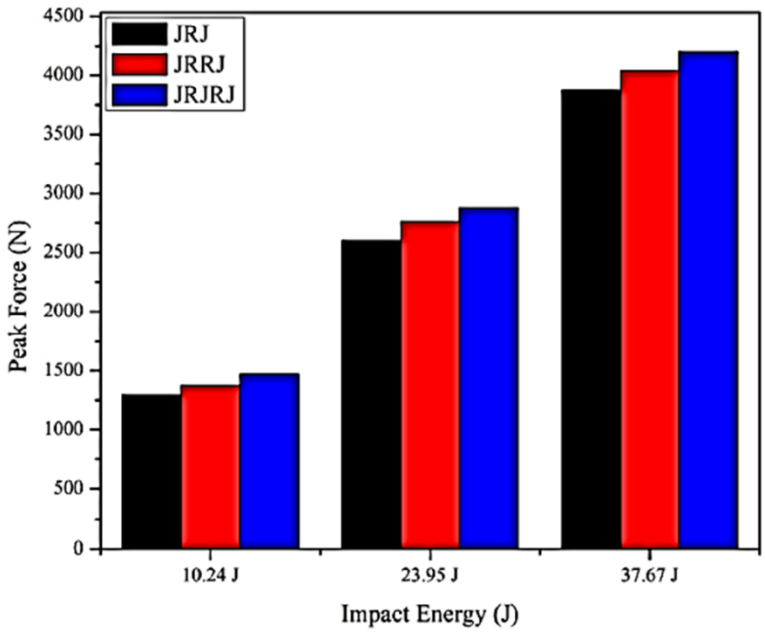

Fig. 21 Flexible composites peak force at different impact energies [215]. Reprinted with permission from ref. 215 (Copyright © 2019 Elsevier).

Khodadadi et al. [96] studied Kevlar/rubber composites in terms of impact resistance. They employed low-hardness (LH) and high-hardness (HH) rubber matrixes. They compared the high-velocity impact behavior of the composites to the impact behavior of Kevlar/epoxy composites in order to explore the influence of a hard, brittle

matrix in comparison to a soft, flexible one on composite energy absorption. Fig. 22 illustrates the ballistic limits of the double- and four-layered composites. According to Fig. 22, the LH and HH rubber matrix specimens exhibited improved ballistic limits in comparison to the neat double- and four-layered fabrics. Kevlar fabric and rubber matrix composites enjoy significant ballistic behavior in light of the great damping properties of rubber. Rubber attaches layers to each other and enables them to exert effective projectile resistance. In contrast, a TS matrix yields an inflexible composite with a negative influence on the ballistic behavior of the fabric.

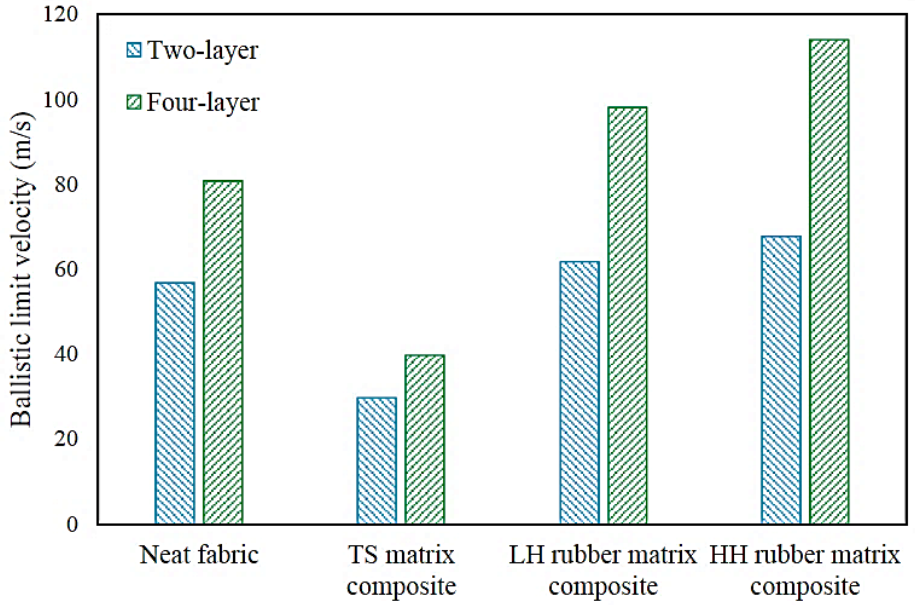

Fig. 22 Ballistic limit of different specimens [96]. Reprinted with permission from ref. 96 (Copyright © 2019 Elsevier).

Fig. 23 compares the TS and HH rubber matrix composites in terms of the impact response under high-velocity impacts. The front and back faces of the composites are demonstrated. The major difference between the rubber and TS matrixes in behavior arises from fabric deformation. The yarns that enable the fabric to exert projectile resistance are not restricted by the rubber matrix. In contrast, solely a small number of yarns resist in the impact area within the TS matrix. This difference results in

a considerable alternation in the ballistic behavior of the composites with rubber and TS matrixes.

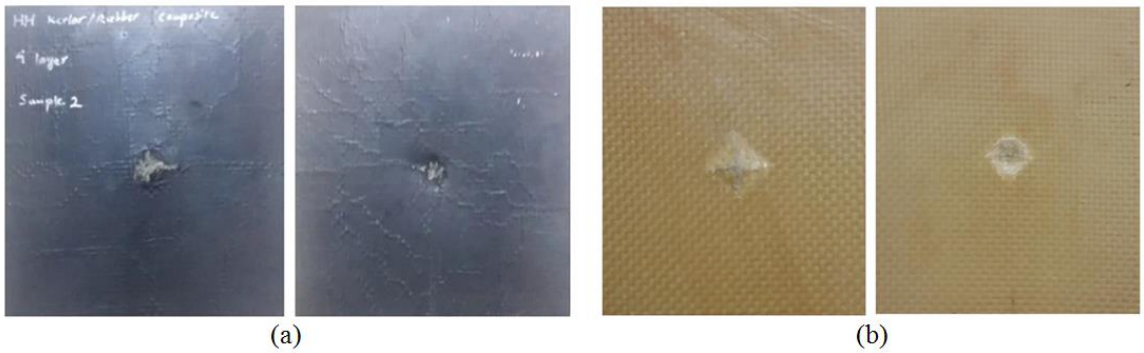

Fig. 23 Front and back face of (a) Rubber matrix composite (b) TS matrix composite[96]. Reprinted with permission from ref. 96 (Copyright © 2019 Elsevier).

Khodadadi et al. [217] proposed a FEM model coupled with experimental tests for the response simulation of neat and rubber matrix composites subjected to impact loads. They individually modeled the warp and weft yarns and incorporated a rubber matrix to fabricate composites. They utilized rubber types with different formulations. Hopkinson pressure bar tests were performed to derive the mechanical properties of the rubbers and introduce them to the model. The Kevlar/rubber composites exhibited higher ballistic performance, and composite integrity was observed after rubber matrix-induced perforation. They also found that the use of rubber in the form of a matrix slightly altered Kevlar fabric flexibility. Two-dimensional drape tests were carried out for the flexibility measurement of fabrics, as shown in Fig. 24. As can be seen, the flexibility of the double-layered Kevlar fabric with a bend angle of 55 degrees and those of the HH and LH Kevlar/rubber composites with the bend angles of 48 and 51 degrees are compared. According to Fig. 24, the neat fabric and composites did not exhibit significant flexibility differences.

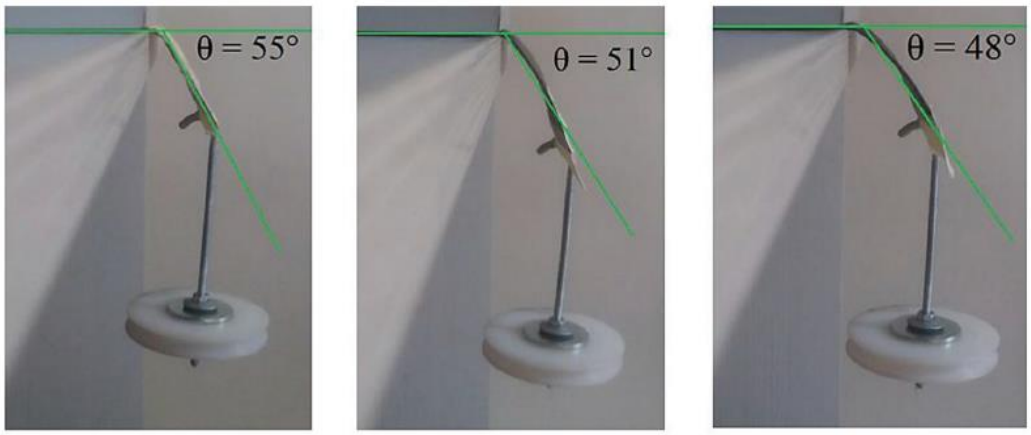

Fig. 24 Drape test (a) Kevlar fabric (b) Kevlar/LH rubber composite (c) Kevlar/HH rubber composite [217]. Reprinted with permission from ref. 217 (Copyright © 2019 Elsevier).

7. Application of an elastomer layer in laminates

Even though the main scope of this review paper was limited to soft composite targets, the other application of elastomer layer is worthy to mention. Due to the unique range of mechanical properties such as low weight, high strength, and excellent damping properties, Elastomers have extensively been used in different structures [218]. Fiber metal laminates (FMLs) are one the considered areas into which elastomers can play an important role. In this section the mechanical properties and impact response of laminates in presence of elastomer layer will be reviewed.

7.1. Mechanical properties of laminates in presence of an elastomeric layer

As for superior properties of carbon fibers, they have become very common in FML structures, however, of coefficients of thermal expansion and the possibility of galvanic corrosion could be a major problem [219]. To overcome these issues, incorporation of elastomeric layers followed by an optimization process to maintain the weight efficiency could be a reasonable solution [220] which results in a structure with

aluminum core and carbon fiber reinforced polymer face sheets with elastomer interlayers.

Thick elastomer interlayers might have a negative impact on the performance of the laminate in terms of lowering the mechanical properties and lightweight potential of the structure [220, 221], therefore, thin elastomeric layers are preferred to tackle these issues as well as maintain the desired interfacial properties [222]. Studies have demonstrated that although the interfacial shear strength is independent from the elastomer thickness, flexural stiffness increased by an amount of 300% by reducing EPDM rubber thickness from 0.5 to 0.1 millimeters [221].

Damping properties of fiber metal laminate structures with different elastomeric layers has also been a matter of concern. Although it has been proven that changing of metal material doesn't have a significant influence on damping properties [223], other parameters such as layup configuration, elastomer thickness and stiffness play prominent roles [224]. It is revealed that the first natural frequency is only affected by the thickness of the elastomer whilst second and higher natural frequencies are functions of the laminate layup as well as elastomer thickness and stiffness as depicted in Fig. 25 [224].

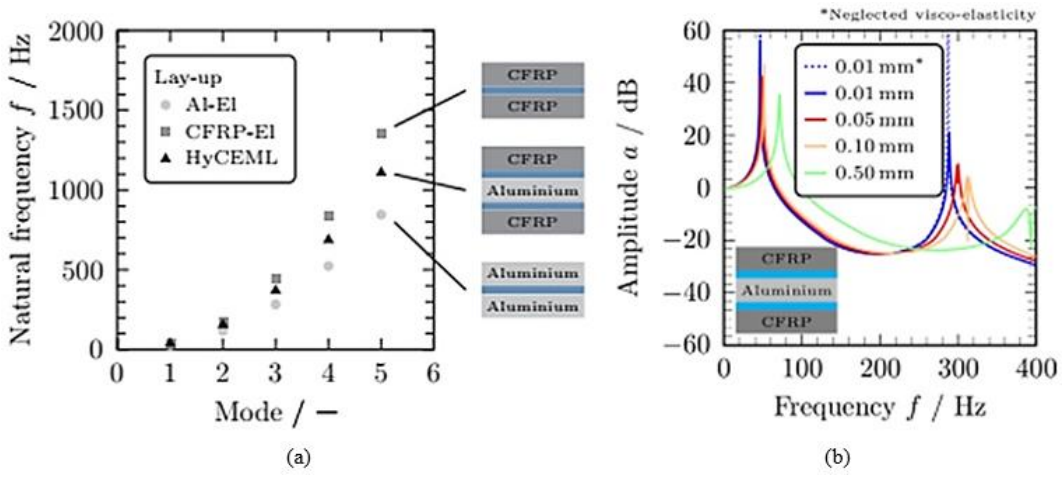

Fig. 25 (a) natural frequencies of several lay-ups and (b) elastomer thickness effect on amplitude [224]. Reprinted with permission from ref. 224 (Copyright © 2018 Elsevier).

In addition to validity of the role of mixtures to obtain the loss factor for elastomer contained laminates, damping capacity of the whole structure has been shown to increase by thickening the elastomer interlayer [225]. Elastomers have also been considered to improve the metal/polymer adhesion in hybrid laminates. Vulcanizing thin EPDM rubber layers in between steel and GFRP composite is shown to be effective in creating high quality interfaces without needing any surface pre-treatments [226]. The assessment of environmental resistance of such a structure under harsh hot/moist environments demonstrates that not only is there no degradation in elastomeric phase but the metal/elastomer and GFRP/elastomer interphases also maintain their properties according to peel tests [227]. In the case of using binding agents in elastomeric laminates, care should be taken to choose proper adhesive based on the engaged adherents and the rate of load application[228].

7.2. Impact response of laminates in presence of elastomer layer

During recent decades, there have been a growing concern in manufacturing structures with high energy absorption capacity and due to the outstanding protective role of elastomeric layers, they have been used in different laminates configurations. One of the studies investigated the high velocity impact response of aluminum/polyurea composites with different layer thicknesses impacted by a full metal jacket (FMJ) projectile [229]. Seven different configurations were considered during which the impact velocity was fixed at 945 m/s while residual velocities were measured by a chronograph. Results demonstrated that application of elastomeric layers contributed positively in improving the velocity reduction per unit areal density of the laminate. In addition, using a thicker elastomeric layer on the back face of the laminate was shown to be much more effective than the other configurations. In similar study, numerical and

analytical approaches were chosen to assess the impact resistance of this structure [230]. High strain rate properties of the constituents were obtained through the split Hopkinson pressure bar tests and the simulation of penetration process was performed using advanced finite element code LS-DYNA. Damage mechanisms and residual velocities were captured accurately as it was expected through experimental studies (Fig. 26).

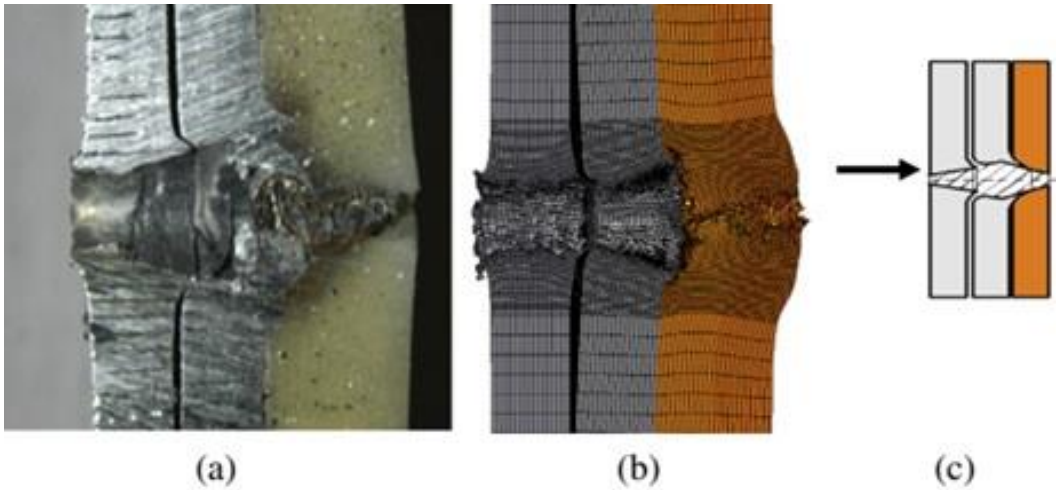

Fig. 26 Aluminum/polyurea composites under impact loading (a) experimental results, (b) numerical simulation and (c) schematic representation [230]. Reprinted with permission from ref. 230 (Copyright © 2015 Elsevier).

In addition to aluminum, steel plates have also been studied along with elastomers [231]. Three kinds of configurations including blank steel plate, steel plate backed by a layer of polyurea and sandwich panels made of steel face sheets and polyurea core were investigated. Results demonstrated that, in contrary to the flat projectile, when pointed projectile hits the polyurea backed plate, the polyurea backing contributes positively in delaying the fracture of steel plate as more energy is dissipated than the blank plate during the shaded area (Fig. 27). Besides, polyurea core in sandwich structure was shown to be less effective than the backing layer.

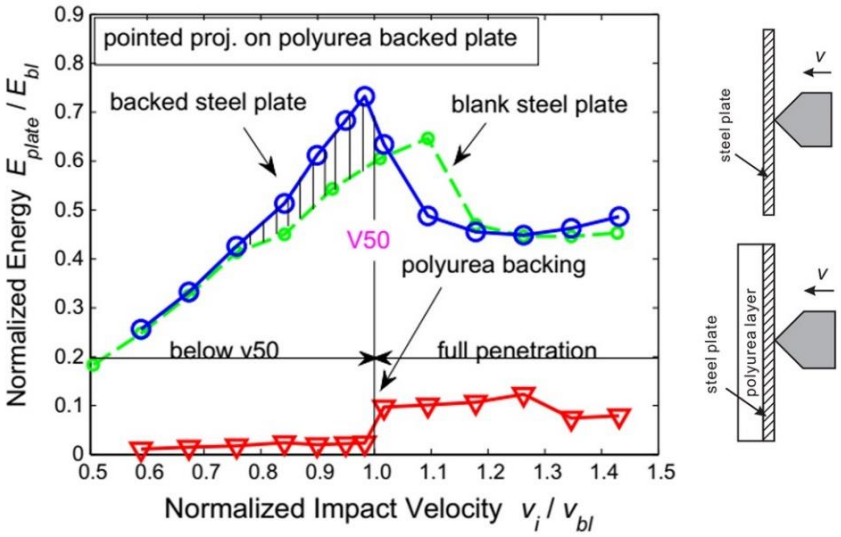

Fig. 27 Energy absorption of blank steel plates and the polyurea backing [231]. Reprinted with permission from ref. 231 (Copyright © 2010 Elsevier).

Another study is dedicated to the steel substrates incorporating a front face laminate [196], the latter consists of alternating layers of thin metal and polyurea elastomer. Results showed that using an eight-layer laminate in the front face of a steel substrate is preferable than the elastomer coated steel bilayer at the same areal density (Fig. 28) as well as changing of the laminate metal to titanium had a minimal effect on perforation performance.

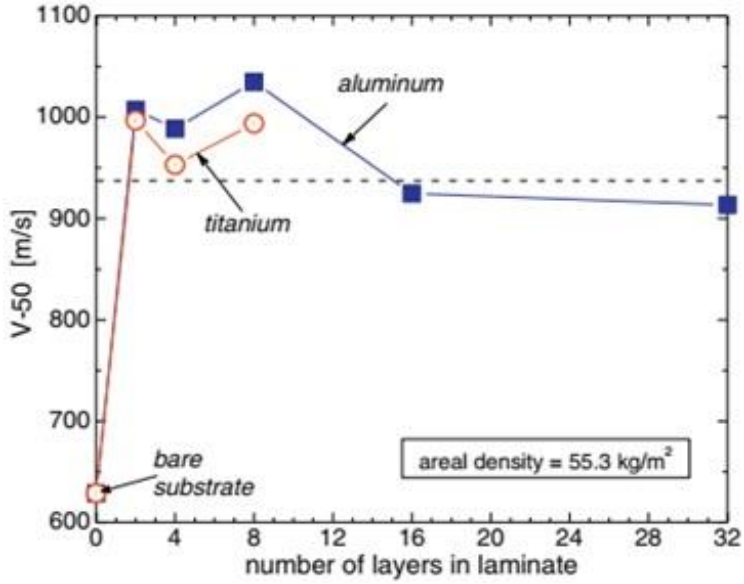

Fig. 28 Perforation performance for a 5.3 mm steel substrate with different frontal laminate configurations [196]. Reprinted with permission from ref. 196 (Copyright © 2016 Elsevier).

Elastomer-coated metal substrates have also been of significant interest. To investigate the effect of rubber characteristics on perforation resistance, polybutadiene (PB) and polyurea (PU) were applied to 5.1 mm thick steel plates at the front face [232]. It was observed that the polyurea exhibited a better performance at high strain rates which can be attributed to a viscoelastic phase transition. Indeed, while the PB segmental dynamics are faster than the applied strain rate, for PU these motions are in order of this rate of deformation, therefore, a transition to glassy state occurs in PU which leads to a brittle failure (Fig. 29) and more energy dissipation.

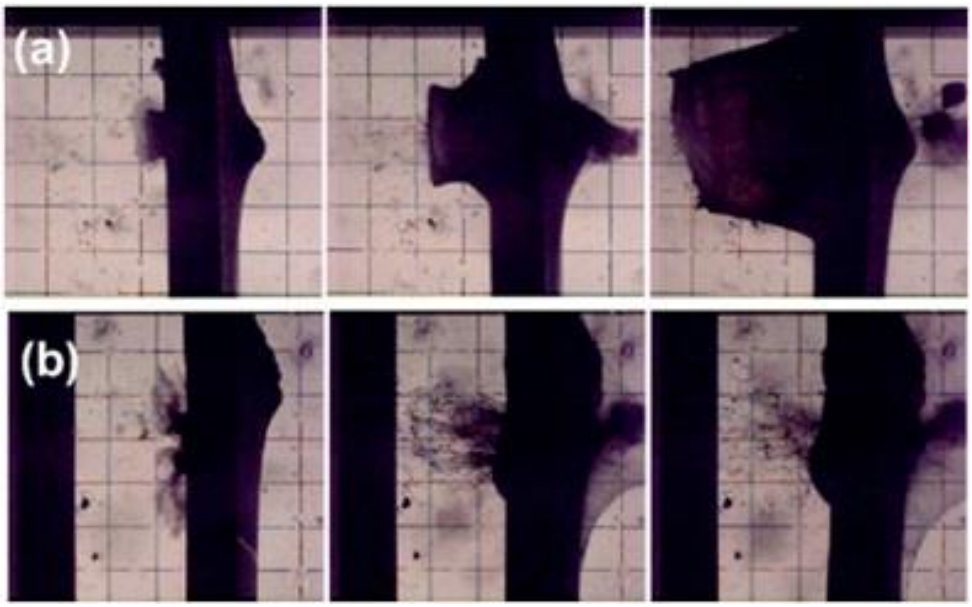

Fig. 29 High speed photos of the perforation process (a) rubbery behavior of polybutadiene and (b) glass transition and brittle failure in polyurea[232]. Reprinted with permission from ref. 232 (Copyright © 2007 API)

Another study has also dedicated to investigate the factors influencing the behavior of such a structure [233]. The results revealed that the coating performance is coupled to the mechanical properties of the substrate such that as the hardness of the substrate increases, the contribution of the elastomer coating is more pronounced, besides, nanoparticle fillers were proved to have a modest effect on ballistic performance of polyurea. A numerical simulation on the deformation-induced glass

transition phenomenon showed that the failure mode of the elastomer is a function of the difference between the test temperature and the elastomer glass transition temperature [234]. At low temperature differences, elastomer tends to transform into its glassy-state during deformation.

Interfacial bonding strength could also be a critical parameter in the impact response of metal/elastomer bilayers. To assess this issue, natural compounded rubber was applied on thin layers of aluminum and the structure was perforated at different impact velocities [235]. A validated numerical model was used to investigate the prominent parameters. As illustrated in Fig. 30, by increasing the interfacial bonding strength between rubber and aluminum, the energy absorption capacity decreases. Besides, there is a critical impact velocity above and below which the aluminum plate with elastomer in front (FF) and back face (BF) absorb higher amount of energy, respectively. The ballistic limit of the bilayer was also shown to improve by increasing the rubber hardness.

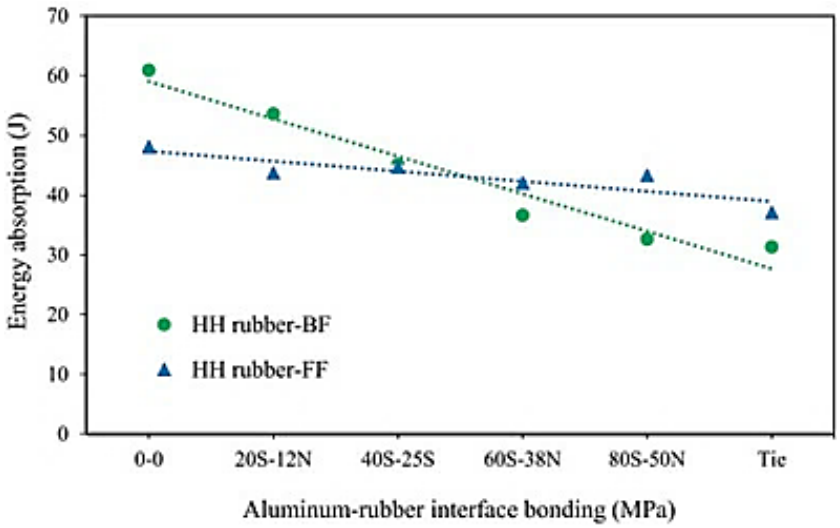

Fig. 30 Energy absorption of Al/rubber bilayer plates with different interfacial strengths [235]. Reprinted with permission from ref. 235 (Copyright © 2020 Elsevier).

Low velocity impact response of elastomer/aluminum bilayers has also investigated [236]. It was demonstrated that not only does an elastomeric layer improve the energy absorbing capacity, but it also reduces the permanent plastic deformation of the whole structure.In addition to bilayers, elastomeric materials have been used to improve the impact properties of more complicated structures such as fiber metal laminates. To do so, an experimental and numerical study was accomplished through incorporating a compounded rubber layer into the commercial glass laminate aluminum reinforced epoxy (GLARE), as depicted in Fig. 31(a), to investigate the impact response of such structure [237]. Results demonstrated that owing to the ability of elastomer in spreading the impact load on a wider area, an elastomeric layer located nearer to the frontal face could be more efficient. Furthermore, the more the impact velocity increases, the better the energy absorption efficiency would become since a wider region could be engaged in damage area (Fig. 31(b)).

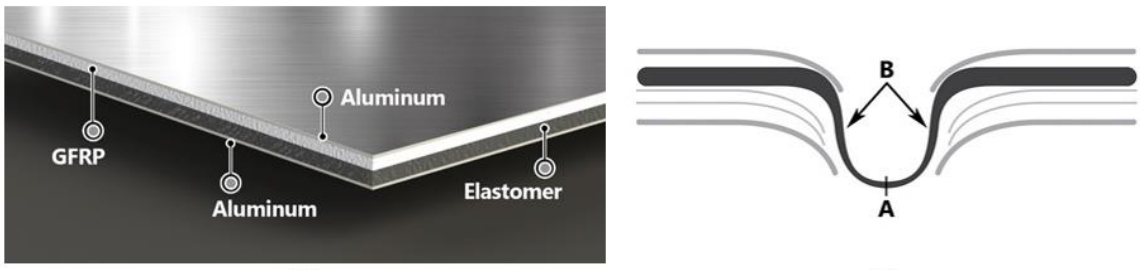

Fig. 31 (a) Configuration of the elastomer layered fiber metal laminate (EFML) structure (b) Movement of the damage initiation point of the elastomer from A to B by increasing the impact velocity [237]. Reprinted with permission from ref. 237 (Copyright © 2020 Elsevier).

High velocity impact response of a layered steel/rubber/composite structure has also been investigated [238]. It was revealed that although the amount of absorbed energy did not change by using an elastomeric layer, the area of permanent damage decreased by nearly 50%. It is worth to mention that whilst the damage area was

independent of the elastomer thickness within a range of 0.5-1.5 mm, it was dependent on the impact energy.

Overall, introducing elastomeric layers into conventional laminates could be beneficial from different viewpoints. Locating as a frontal coating, elastomer would be capable of either spreading the exerted impact load or undergoing viscoelastic phase transition which both contribute positively to perforation performance. Besides, as a back layer, it could curb the projectile motion via stretching until its failure. From a damage point of view, an elastomeric layer would reduce the permanent plastic deformation of the whole structure or delay the damage initiation within the other engaged layers.

Conclusion

In this study, the impact resistance of soft targets was reviewed. Energy absorption mechanisms of high-performance fabric and parameters that affect the impact resistance of fabrics such as material properties, fabric structure, friction, projectile geometry, pre-tension and boundary condition were studied. Although ballistic fabrics have high capacity to absorb energy but adding soft matrices to woven fabric enhances the ballistic performance of fabrics. Shear thickening fluids and theories to explain shear thickening mechanism, as well as important factors that affect the rheological behavior of shear thickening fluids were reviewed. The use of shear thickening fluids has shown hopeful results against impact loading based on publications in literature conducted numerically and experimentally. Although some researchers have stated the impact resistance improvement of STF/fabric composite is related to shear thickening effect but increase in friction between yarns was regarded as the primary contribution of shear thickening fluid under impact loading in many researches.

Elastomers with high damping characteristics and high flexibility make fabric/elastomer composites a good candidate for blast and ballistic applications. In addition, better performance can be attributed to the primary yarns that remain in contact with the projectile surface area during penetration and perforation compared to neat fabric. Furthermore, the possible application of elastomeric layer used to manufacture a composite laminate was reviewed. According to literature, using elastomeric layers contributed positively in improving the impact resistance of composite laminates. Moreover, positioning the elastomeric layer affect the ballistic performance of a composite significantly.

As mentioned, both natural rubber and shear thickening fluid improve the impact performance of fabrics. Indeed, friction enhancement is the main source of performance improvement in fabric/STF and Fabric/NR composites. Despite the flexibility of these composites, the rubber matrix causes a slight drop in the flexibility of the fabric, which, in turn, affect the performance of fabric by restraining the yarns movement. On the other hand, however, rubber with high damping properties contributes positively to dissipating projectile's energy. Further investigation and quantitative verification is necessary to compare soft matrices and their hybrid arrangements in high-performance composites. The importance of developing rather accurate analytical formulations in elastomer layered structures is more pronounced, provided that exact interactions and damage mechanisms are to be explored.

References

[1] Srivastava A, Majumdar A, Butola B. Improving the impact resistance of textile structures by using shear thickening fluids: a review. Critical Reviews in Solid State and Materials Sciences. 2012;37:115-29.

[2] Khoda-Rahmi H, Fallahi A, Liaghat G. Incremental deformation and penetration analysis of deformable projectile into semi-infinite target. International Journal of Solids and Structures. 2006;43:569-82.

[3] Fras T, Roth CC, Mohr D. Fracture of high-strength armor steel under impact loading. International Journal of Impact Engineering. 2018;111:147-64.

[4] Khazraiyan N, Liaghat GH, Khodarahmi H. Normal impact of hard projectiles on concrete targets. Structural Concrete. 2013;14:176-83.

[5] Bayat A, Liaghat G, Sabouri H, Ashkezari GD, Pedram E, Taghizadeh SA, et al. Experimental investigation on the quasi-static mechanical behavior of autoclaved aerated concrete insulated sandwich panels. Journal of Sandwich Structures & Materials. 2019:1099636219857633.

[6] Bayat A, Liaghat GH, Ghalami-Choobar M, Ashkezari GD, Sabouri H. Analytical modeling of the high-velocity impact of autoclaved aerated concrete (AAC) blocks and some experimental results. International Journal of Mechanical Sciences. 2019;159:315-24.

[7] Ryan S, Li H, Edgerton M, Gallardy D, Cimpoeru S. The ballistic performance of an ultra-high hardness armour steel: An experimental investigation. International Journal of Impact Engineering. 2016;94:60-73.

[8] Ahmadi H, Liaghat G, Sabouri H, Bidkhouri E. Investigation on the high velocity impact properties of glass-reinforced fiber metal laminates. Journal of Composite Materials. 2013;47:1605-15.

[9] Tian C, An X, Sun Q, Dong Y. Experimental and numerical analyses of the penetration resistance of ceramic-metal hybrid structures. Composite Structures. 2019;211:264-72.

[10] Tahmaseiabdar M, Liaghat GH, Shanazari H, Khodadadi A, Hadavinia H, Abotorabi A. Analytical and numerical investigation of projectile perforation into ceramic-metal targets and presenting a modified theory. Modares Mechanical Engineering. 2015;15:353-9.

[11] Bresciani L, Manes A, Giglio M. An analytical model for ballistic impacts against ceramic tiles. Ceramics International. 2018;44:21249-61.

[12] Medvedovski E. Ballistic performance of armour ceramics: Influence of design and structure. Part 2. Ceramics International. 2010;36:2117-27.

[13] Ahmadi H, Liaghat G, Charandabi SC. High velocity impact on composite sandwich panels with nano-reinforced syntactic foam core. Thin-Walled Structures. 2020;148:106599.

[14] Ahmadi H, Liaghat G. Analytical and experimental investigation of high velocity impact on foam core sandwich panel. Polymer Composites. 2019;40:2258-72.

[15] Hassanpour Roudbeneh F, Liaghat G, Sabouri H, Hadavinia H. Experimental investigation of quasistatic penetration tests on honeycomb sandwich panels filled with polymer foam. Mechanics of Advanced Materials and Structures. 2018:1-13.

[16] Hassanpour Roudbeneh F, Liaghat G, Sabouri H, Hadavinia H. Experimental investigation of impact loading on honeycomb sandwich panels filled with foam. International Journal of Crashworthiness. 2019;24:199-210.

[17] Mawkhlieng U, Majumdar A. Soft body armour. Textile Progress. 2019;51:139-224.

[18] Shanazari H, Liaghat G, Hadavinia H, Aboutorabi A. Analytical investigation of high-velocity impact on hybrid unidirectional/woven composite panels. Journal of Thermoplastic Composite Materials. 2017;30:545-63.
[19] Yeganeh EM, Liaghat G, Pol M. Laminate composites behavior under quasi-static and high velocity perforation. Steel and Composite Structures. 2016;22:777-96.
[20] Palta E, Fang H. On a multi-scale finite element model for evaluating ballistic performance of multi-ply woven fabrics. Composite Structures. 2019;207:488-508.
[21] Bajya M, Majumdar A, Butola BS, Arora S, Bhattacharjee D. Ballistic performance and failure modes of woven and unidirectional fabric based soft armour panels. Composite Structures. 2021;255:112941.
[22] Dimeski D, Srebrenkoska V, Mirceska N. Ballistic impact resistance mechanism of woven fabrics and their composites. International Journal of Engineering Research & Technology (IJERT). 2015;4:107-12.
[23] Khodadadi A, LIAGHAT GH, Akbari M, Tahmasebi M. Numerical and experimental analysis of penetration into Kevlar fabrics and investigation of the effective factors on the ballistic performance. Modares Mechanical Engineering. 2014;13:124-133.
[24] Wagner N, Wetzel ED. Advanced body armor utilizing shear thickening fluids. Google Patents; 2009.
[25] Majumdar A, Butola BS, Srivastava A, Bhattacharjee D, Biswas I, Laha A, et al. Improving the impact resistance of p-aramid fabrics by sequential impregnation with shear thickening fluid. Fibers and Polymers. 2016;17:199-204.
[26] Yang H, Yao X-F, Wang S, Ke Y-C, Huang S-H, Liu Y-H. Analysis and inversion of contact stress for the finite thickness Neo-Hookean layer. Journal of Applied Mechanics. 2018;85.
[27] Tubaldi E, Mitoulis S, Ahmadi H. Comparison of different models for high damping rubber bearings in seismically isolated bridges. Soil Dynamics and Earthquake Engineering. 2018;104:329-45.
[28] Yang H, Yao X, Zheng Z, Gong L, Yuan L, Yuan Y, et al. Highly sensitive and stretchable graphene-silicone rubber composites for strain sensing. Composites Science and Technology. 2018;167:371-8.
[29] Pouriayevali H, Guo Y, Shim V. A visco-hyperelastic constitutive description of elastomer behaviour at high strain rates. Procedia Engineering. 2011;10:2274-9.
[30] Mamivand M, Liaghat G. A model for ballistic impact on multi-layer fabric targets. International Journal of Impact Engineering. 2010;37:806-12.
[31] Chu T-L, Ha-Minh C, Imad A. A numerical investigation of the influence of yarn mechanical and physical properties on the ballistic impact behavior of a Kevlar KM2® woven fabric. Composites Part B: Engineering. 2016;95:144-54.
[32] Kędzierski P, Popławski A, Gieleta R, Morka A, Sławiński G. Experimental and numerical investigation of fabric impact behavior. Composites Part B: Engineering. 2015;69:452-9.
[33] Moure M, Rubio I, Aranda-Ruiz J, Loya J, Rodríguez-Millán M. Analysis of impact energy absorption by lightweight aramid structures. Composite Structures. 2018;203:917-26.
[34] Nilakantan G, Nutt S. Effects of ply orientation and material on the ballistic impact behavior of multilayer plain-weave aramid fabric targets. Defence technology. 2018;14:165-78.
[35] Zhenhua Z, Lulu L, Wei C, Gang L. Numerical simulation methodology of multi-layer Kevlar 49 woven fabrics in aircraft engine containment application. International Journal of Crashworthiness. 2019;24:86-99.
[36] Fahool M, Sabet AR. Parametric study of energy absorption mechanism in Twaron fabric impregnated with a shear thickening fluid. International Journal of Impact Engineering. 2016;90:61-71.
[37] Yang Y, Chen X. Influence of fabric architecture on energy absorption efficiency of soft armour panel under ballistic impact. Composite Structures. 2019;224:111015.
[38] Yang Y, Chen X. Investigation on energy absorption efficiency of each layer in ballistic armour panel for applications in hybrid design. Composite Structures. 2017;164:1-9.
[39] Bilisik K. Two-dimensional (2D) fabrics and three-dimensional (3D) preforms for ballistic and stabbing protection: A review. Textile Research Journal. 2017;87:2275-304.

[40] Yuan Z, Chen X, Zeng H, Wang K, Qiu J. Identification of the elastic constant values for numerical simulation of high velocity impact on dyneema® woven fabrics using orthogonal experiments. Composite Structures. 2018;204:178-91.
[41] Wang H, Hazell PJ, Shankar K, Morozov EV, Escobedo JP, Wang C. Effects of fabric folding and thickness on the impact behaviour of multi-ply UHMWPE woven fabrics. Journal of materials science. 2017;52:13977-91.
[42] Gürgen S, Kuşhan MC. High performance fabrics in body protective systems. Materials Science Forum. 2017;880:132-135.
[43] Huang Y, Frings P, Hennes E. Mechanical properties of Zylon/epoxy composite. Composites Part B: Engineering. 2002;33:109-15.
[44] Pereira JM, Revilock Jr DM. Ballistic impact response of Kevlar 49 and Zylon under conditions representing jet engine fan containment. Journal of Aerospace Engineering. 2009;22:240-8.
[45] Holmes GA, Rice K, Snyder CR. Ballistic fibers: a review of the thermal, ultraviolet and hydrolytic stability of the benzoxazole ring structure. Journal of materials science. 2006;41:4105-16.
[46] Cunniff PM. An analysis of the system effects in woven fabrics under ballistic impact. Textile Research Journal. 1992;62:495-509.
[47] Yang Y, Chen X. Investigation of energy absorption mechanisms in a soft armor panel under ballistic impact. Textile Research Journal. 2017;87:2475-86.
[48] Shaktivesh, Nair N, Naik N. Ballistic impact behavior of 2D plain weave fabric targets with multiple layers: Analytical formulation. International Journal of Damage Mechanics. 2015;24:116-50.
[49] Manimala JM, Sun C. Investigation of failure in Kevlar fabric under transverse indentation using a homogenized continuum constitutive model. Textile Research Journal. 2014;84:388-98.
[50] Tabiei A, Nilakantan G. Ballistic impact of dry woven fabric composites: a review. Applied Mechanics Reviews. 2008;61.
[51] Nilakantan G, Merrill RL, Keefe M, Gillespie Jr JW, Wetzel ED. Experimental investigation of the role of frictional yarn pull-out and windowing on the probabilistic impact response of kevlar fabrics. Composites Part B: Engineering. 2015;68:215-29.
[52] Cheeseman BA, Bogetti TA. Ballistic impact into fabric and compliant composite laminates. Composite Structures. 2003;61:161-73.
[53] Mawkhlieng U, Majumdar A, Laha A. A review of fibrous materials for soft body armour applications. RSC Advances. 2020;10:1066-86.
[54] McCrackin FL, Schiefer HF, Smith JC, Stone WK. Stress-strain relationships in yarns subjected to rapid impact loading: part II. Breaking velocities, strain energies, and theory neglecting wave propagation. Textile Research Journal. 1955;25:529-34.
[55] Rao M, Duan Y, Keefe M, Powers B, Bogetti T. Modeling the effects of yarn material properties and friction on the ballistic impact of a plain-weave fabric. Composite Structures. 2009;89:556-66.
[56] Ha-Minh C, Imad A, Boussu F, Kanit T, Crepin D. Numerical study on the effects of yarn mechanical transverse properties on the ballistic impact behaviour of textile fabric. The Journal of Strain Analysis for Engineering Design. 2012;47:524-34.
[57] Nilakantan G, Keefe M, Wetzel ED, Bogetti TA, Gillespie Jr JW. Effect of statistical yarn tensile strength on the probabilistic impact response of woven fabrics. Composites Science and Technology. 2012;72:320-9.
[58] Yang C, Tran P, Ngo T, Mendis P, Humphries W. Effect of textile architecture on energy absorption of woven fabrics subjected to ballistic impact. Applied Mechanics and Materials: Trans Tech Publ; 2014. p. 757-62.
[59] Zhou Y, Chen X. A numerical investigation into the influence of fabric construction on ballistic performance. Composites Part B: Engineering. 2015;76:209-17.
[60] Beliaev A, Beliakova T, Chistyakov P, Iniukhin A, Kostyreva L, Mossakovsky P, et al. The influence of the weaving pattern on the interface friction in aramid fabrics under the

conditions of the transverse loading. International Journal of Mechanical Sciences. 2018;145:120-7.
[61] Tran P, Ngo T, Yang E, Mendis P, Humphries W. Effects of architecture on ballistic resistance of textile fabrics: Numerical study. International Journal of Damage Mechanics. 2014;23:359-76.
[62] Yang C-C, Ngo T, Tran P. Influences of weaving architectures on the impact resistance of multi-layer fabrics. Materials & Design. 2015;85:282-95.
[63] Özdemir H, Mert E. The effects of fabric structural parameters on the tensile, bursting, and impact strengths of cellular woven fabrics. Journal of the Textile Institute. 2013;104:330-8.
[64] Gu B. Modelling of 3D woven fabrics for ballistic protection. Advanced Fibrous Composite Materials for Ballistic Protection: Elsevier; 2016. p. 145-97.
[65] Ma P, Jin L, Wu L. Experimental and numerical comparisons of ballistic impact behaviors between 3D angle-interlock woven fabric and its reinforced composite. Journal of Industrial Textiles. 2019;48:1044-58.
[66] Ha-Minh C, Imad A, Boussu F, Kanit T. Experimental and numerical investigation of a 3D woven fabric subjected to a ballistic impact. International Journal of Impact Engineering. 2016;88:91-101.
[67] Saleh MN, Soutis C. Recent advancements in mechanical characterisation of 3D woven composites. Mechanics of Advanced Materials and Modern Processes. 2017;3:12.
[68] Karaduman NS, Karaduman Y, Ozdemir H, Ozdemir G. Textile reinforced structural composites for advanced applications. Textiles for advanced applications. 2017:87.
[69] Chu T-L, Ha-Minh C, Imad A. Analysis of local and global localizations on the failure phenomenon of 3D interlock woven fabrics under ballistic impact. Composite Structures. 2017;159:267-77.
[70] Ren C, Liu T, Siddique A, Sun B, Gu B. High-speed visualizing and mesoscale modeling for deformation and damage of 3D angle-interlock woven composites subjected to transverse impacts. International Journal of Mechanical Sciences. 2018;140:119-32.
[71] Chu Y, Min S, Chen X. Numerical study of inter-yarn friction on the failure of fabrics upon ballistic impacts. Materials & Design. 2017;115:299-316.
[72] Wang Y, Miao Y, Huang L, Swenson D, Yen C-F, Yu J, et al. Effect of the inter-fiber friction on fiber damage propagation and ballistic limit of 2-D woven fabrics under a fully confined boundary condition. International Journal of Impact Engineering. 2016;97:66-78.
[73] Khodadadi A lG, Tahmasebi M, Hadavinia H. Investigation of the Effect of Friction on the Ballistic performance of Fabric Targets. Biennial International Conference on Experimental Solid Mechanics. 2014.
[74] Briscoe B, Motamedi F. The ballistic impact characteristics of aramid fabrics: the influence of interface friction. Wear. 1992;158:229-47.
[75] Bazhenov S, Goncharuk G. The influence of water on the friction forces of fibers in aramid fabrics. Polymer Science Series A. 2014;56:184-95.
[76] Zhou Y, Chen X, Wells G. Influence of yarn gripping on the ballistic performance of woven fabrics from ultra-high molecular weight polyethylene fibre. Composites Part B: Engineering. 2014;62:198-204.
[77] Khodadadi A, Liaghat G, Vahid S, Sabet A, Hadavinia H. Ballistic performance of Kevlar fabric impregnated with nanosilica/PEG shear thickening fluid. Composites Part B: Engineering. 2019;162:643-52.
[78] Wang Y, Chen X, Young R, Kinloch I. Finite element analysis of effect of inter-yarn friction on ballistic impact response of woven fabrics. Composite Structures. 2016;135:8-16.
[79] Das S, Jagan S, Shaw A, Pal A. Determination of inter-yarn friction and its effect on ballistic response of para-aramid woven fabric under low velocity impact. Composite Structures. 2015;120:129-40.
[80] Nilakantan G, Wetzel ED, Bogetti TA, Gillespie Jr JW. Finite element analysis of projectile size and shape effects on the probabilistic penetration response of high strength fabrics. Composite Structures. 2012;94:1846-54.

[81] Nilakantan G, Wetzel ED, Bogetti TA, Gillespie Jr JW. A deterministic finite element analysis of the effects of projectile characteristics on the impact response of fully clamped flexible woven fabrics. Composite Structures. 2013;95:191-201.
[82] Talebi H, Wong S, Hamouda A. Finite element evaluation of projectile nose angle effects in ballistic perforation of high strength fabric. Composite Structures. 2009;87:314-20.
[83] Hudspeth M, Chu J-m, Jewell E, Lim B, Ytuarte E, Tsutsui W, et al. Effect of projectile nose geometry on the critical velocity and failure of yarn subjected to transverse impact. Textile Research Journal. 2017;87:953-72.
[84] Tapie E, Tan E, Guo Y, Shim V. Effects of pre-tension and impact angle on penetration resistance of woven fabric. International Journal of Impact Engineering. 2017;106:171-90.
[85] Lulu L, Zhenhua Z, Wei C, Gang L. Influence of pre-tension on ballistic impact performance of multi-layer Kevlar 49 woven fabrics for gas turbine engine containment systems. Chinese Journal of Aeronautics. 2018;31:1273-86.
[86] Nilakantan G, Gillespie Jr JW. Yarn pull-out behavior of plain woven Kevlar fabrics: Effect of yarn sizing, pullout rate, and fabric pre-tension. Composite Structures. 2013;101:215-24.
[87] Guo G. Finite element analysis of pre-stretch effects on ballistic impact performance of woven fabrics. Composite Structures. 2018;200:173-86.
[88] Nilakantan G, Gillespie Jr JW. Ballistic impact modeling of woven fabrics considering yarn strength, friction, projectile impact location, and fabric boundary condition effects. Composite Structures. 2012;94:3624-34.
[89] Gürgen S. The influence of boundary condition on the impact behavior of high performance fabrics. Advanced Engineering Forum. 2018; 28:47-54.
[90] Duan Y, Keefe M, Bogetti T, Powers B. Finite element modeling of transverse impact on a ballistic fabric. International Journal of Mechanical Sciences. 2006;48:33-43.
[91] Arora S, Ghosh A. Evolution of soft body armor. Advanced Textile Engineering Materials. 2018:499-552.
[92] Hedayatian M, Liaghat G, Rahimi G, Pol M, Hadavinia H, Zamani R. Investigation of the high velocity impact behavior of grid cylindrical composite structures. Polymer Composites. 2017;38:2603-8.
[93] Khodadadi A, Liaghat G, Ahmadi H, Bahramian AR, Shahgholian D, Anani Y, et al. Experimental and numerical analysis of high velocity impact on Kevlar/Epoxy composite plates. Journal of Science and Technology of Composites. 2019;6:265-74.
[94] Moeinifard M, Liaghat G, Rahimi G, Talezadehlari A, Hadavinia H. Experimental investigation on the energy absorption and contact force of unstiffened and grid-stiffened composite cylindrical shells under lateral compression. Composite Structures. 2016;152:626-36.
[95] Domun N, Hadavinia H, Zhang T, Sainsbury T, Liaghat G, Vahid S. Improving the fracture toughness and the strength of epoxy using nanomaterials–a review of the current status. Nanoscale. 2015;7:10294-329.
[96] Khodadadi A, Liaghat G, Bahramian AR, Ahmadi H, Anani Y, Asemani S, et al. High velocity impact behavior of Kevlar/rubber and Kevlar/epoxy composites: A comparative study. Composite Structures. 2019;216:159-67.
[97] Arora S, Majumdar A, Butola BS. Deciphering the structure-induced impact response of ZnO nanorod grafted UHMWPE woven fabrics. Thin-Walled Structures. 2020;156:106991.
[98] Chu Y, Chen X, Sheel DW, Hodgkinson JL. Surface modification of aramid fibers by atmospheric pressure plasma-enhanced vapor deposition. Textile Research Journal. 2014;84:1288-97.
[99] Sun D, Chen X. Plasma modification of Kevlar fabrics for ballistic applications. Textile Research Journal. 2012;82:1928-34.
[100] Kim Y, Kumar SKS, Park Y, Kwon H, Kim C-G. High-velocity impact onto a high-frictional fabric treated with adhesive spray coating and shear thickening fluid impregnation. Composites Part B: Engineering. 2020;185:107742.

[101] Gürgen S, Majumdar A. Tuning the frictional properties of carbon fabrics using boron carbide particles. Fibers and Polymers. 2019;20:725-31.
[102] Gürgen S, Yıldız T. Stab resistance of smart polymer coated textiles reinforced with particle additives. Composite Structures. 2020;235:111812.
[103] Pinto F, Meo M. Design and manufacturing of a novel shear thickening fluid composite (STFC) with enhanced out-of-plane properties and damage suppression. Applied Composite Materials. 2017;24:643-60.
[104] Lee YS, Wagner NJ. Rheological properties and small-angle neutron scattering of a shear thickening, nanoparticle dispersion at high shear rates. Industrial & engineering chemistry research. 2006;45:7015-24.
[105] Ding J, Tracey PJ, Li W, Peng G, Whitten PG, Wallace GG. Review on shear thickening fluids and applications. Textiles and Light Industrial Science and Technology (TLIST). 2013; 2:161-173.
[106] Wagner NJ, Wetzel ED. Advanced body armor utilizing shear thickening fluids. Google Patents; 2007.
[107] Hoffman R. Discontinuous and dilatant viscosity behavior in concentrated suspensions. I. Observation of a flow instability. Transactions of the Society of Rheology. 1972;16:155-73.
[108] Hoffman R. Discontinuous and dilatant viscosity behavior in concentrated suspensions. II. Theory and experimental tests. Journal of Colloid and Interface Science. 1974;46:491-506.
[109] Bossis G, Brady J. The rheology of Brownian suspensions. The Journal of chemical physics. 1989;91:1866-74.
[110] Mewis J, Wagner NJ. Colloidal suspension rheology: Cambridge University Press, 2012.
[111] Kalman DP, Wagner NJ. Microstructure of shear-thickening concentrated suspensions determined by flow-USANS. Rheologica acta. 2009;48:897-908.
[112] Maranzano BJ, Wagner NJ. Flow-small angle neutron scattering measurements of colloidal dispersion microstructure evolution through the shear thickening transition. The Journal of chemical physics. 2002;117:10291-302.
[113] Seto R, Mari R, Morris JF, Denn MM. Discontinuous shear thickening of frictional hard-sphere suspensions. Physical review letters. 2013;111:218301.
[114] Mari R, Seto R, Morris JF, Denn MM. Shear thickening, frictionless and frictional rheologies in non-Brownian suspensions. Journal of Rheology. 2014;58:1693-724.
[115] Gürgen S, Li W, Kuşhan MC. The rheology of shear thickening fluids with various ceramic particle additives. Materials & Design. 2016;104:312-9.
[116] Gürgen S, de Sousa RJA. Rheological and deformation behavior of natural smart suspensions exhibiting shear thickening properties. Archives of Civil and Mechanical Engineering. 2020;20:1-8.
[117] Feng X, Li S, Wang Y, Wang Y, Liu J. Effects of different silica particles on quasi-static stab resistant properties of fabrics impregnated with shear thickening fluids. Materials & Design. 2014;64:456-61.
[118] Ghosh A, Chauhan I, Majumdar A, Butola BS. Influence of cellulose nanofibers on the rheological behavior of silica-based shear-thickening fluid. Cellulose. 2017;24:4163-71.
[119] Gürgen S. Tuning the rheology of nano-sized silica suspensions with silicon nitride particles. Journal of Nano Research. 2019;56: 63-70.
[120] Gürgen S, Sofuoğlu MA, Kuşhan MC. Rheological modeling of multi-phase shear thickening fluid using an intelligent methodology. Journal of the Brazilian Society of Mechanical Sciences and Engineering. 2020;42:1-7.
[121] Gürgen S, Sofuoğlu MA, Kuşhan MC. Rheological compatibility of multi-phase shear thickening fluid with a phenomenological model. Smart Materials and Structures. 2019;28:035027.
[122] Huang W, Wu Y, Qiu L, Dong C, Ding J, Li D. Tuning rheological performance of silica concentrated shear thickening fluid by using graphene oxide. Advances in Condensed Matter Physics. 2015;2015.

[123] Mawkhlieng U, Majumdar A, Bhattacharjee D. Graphene Reinforced Multiphase Shear Thickening Fluid for Augmenting Low Velocity Ballistic Resistance. Fibers and Polymers. 2021;22:213-21.
[124] Ávila AF, de Oliveira AM, Leão SG, Martins MG. Aramid fabric/nano-size dual phase shear thickening fluid composites response to ballistic impact. Composites Part A: Applied Science and Manufacturing. 2018;112:468-74.
[125] Hasanzadeh M, Mottaghitalab V. Tuning of the rheological properties of concentrated silica suspensions using carbon nanotubes. Rheologica acta. 2016;55:759-66.
[126] Wei M, Lv Y, Sun L, Sun H. Rheological properties of multi-walled carbon nanotubes/silica shear thickening fluid suspensions. Colloid and Polymer Science. 2020;298:243-50.
[127] Liu M, Zhang S, Liu S, Cao S, Wang S, Bai L, et al. CNT/STF/Kevlar-based wearable electronic textile with excellent anti-impact and sensing performance. Composites Part A: Applied Science and Manufacturing. 2019;126:105612.
[128] Gürgen S, Kuşhan MC. The effect of silicon carbide additives on the stab resistance of shear thickening fluid treated fabrics. Mechanics of Advanced Materials and Structures. 2017;24:1381-90.
[129] Gürgen S, Kuşhan MC, Li W. The effect of carbide particle additives on rheology of shear thickening fluids. Korea-Australia rheology journal. 2016;28:121-8.
[130] Gürgen S, Kuşhan MC. The stab resistance of fabrics impregnated with shear thickening fluids including various particle size of additives. Composites Part A: Applied Science and Manufacturing. 2017;94:50-60.
[131] Gürgen S, Kuşhan MC. The ballistic performance of aramid based fabrics impregnated with multi-phase shear thickening fluids. Polymer Testing. 2017;64:296-306.
[132] Gürgen S, Kuşhan MC, Li W. Shear thickening fluids in protective applications: a review. Progress in Polymer Science. 2017;75:48-72.
[133] Maranzano BJ, Wagner NJ. The effects of particle size on reversible shear thickening of concentrated colloidal dispersions. The Journal of chemical physics. 2001;114:10514-27.
[134] Asija N, Chouhan H, Gebremeskel SA, Bhatnagar N. Influence of particle size on the low and high strain rate behavior of dense colloidal dispersions of nanosilica. Journal of nanoparticle research. 2017;19:21.
[135] Wei R, Dong B, Wang F, Yang J, Jiang Y, Zhai W, et al. Effects of silica morphology on the shear-thickening behavior of shear thickening fluids and stabbing resistance of fabric composites. Journal of Applied Polymer Science. 2020;137:48809.
[136] Li S, Wang J, Cai W, Zhao S, Wang Z, Wang S. Effect of acid and temperature on the discontinuous shear thickening phenomenon of silica nanoparticle suspensions. Chemical Physics Letters. 2016;658:210-4.
[137] Sahoo SK, Mishra S, Islam E, Nebhani L. Tuning shear thickening behavior via synthesis of organically modified silica to improve impact resistance of Kevlar fabric. Materials Today Communications. 2020;23:100892.
[138] Chu B, Brady AT, Mannhalter BD, Salem DR. Effect of silica particle surface chemistry on the shear thickening behaviour of concentrated colloidal suspensions. Journal of Physics D: Applied Physics. 2014;47:335302.
[139] Petel OE, Ouellet S, Loiseau J, Frost DL, Higgins AJ. A comparison of the ballistic performance of shear thickening fluids based on particle strength and volume fraction. International Journal of Impact Engineering. 2015;85:83-96.
[140] Kalman DP, Merrill RL, Wagner NJ, Wetzel ED. Effect of particle hardness on the penetration behavior of fabrics intercalated with dry particles and concentrated particle− fluid suspensions. ACS applied materials & interfaces. 2009;1:2602-12.
[141] Wu L, Wang J, Jiang Q, Lu Z, Wang W, Lin J-H. Low-velocity impact behavior of flexible sandwich composite with polyurethane grid sealing shear thickening fluid core. Journal of Sandwich Structures & Materials. 2020;22:1274-91.
[142] Liu X-Q, Bao R-Y, Wu X-J, Yang W, Xie B-H, Yang M-B. Temperature induced gelation transition of a fumed silica/PEG shear thickening fluid. RSC Advances. 2015;5:18367-74.

[143] Hasanzadeh M, Mottaghitalab V, Rezaei M. Rheological and viscoelastic behavior of concentrated colloidal suspensions of silica nanoparticles: A response surface methodology approach. Advanced Powder Technology. 2015;26:1570-7.
[144] Balali E, Kordani N, Sadough Vanini A. Response of glass fiber-reinforced hybrid shear thickening fluid (STF) under low-velocity impact. The Journal of The Textile Institute. 2017;108:376-84.
[145] Tapie E, Guo Y, Shim V. Yarn mobility in woven fabrics–a computational and experimental study. International Journal of Solids and Structures. 2016;80:212-26.
[146] Cao S, Pang H, Zhao C, Xuan S, Gong X. The CNT/PSt-EA/Kevlar composite with excellent ballistic performance. Composites Part B: Engineering. 2020;185:107793.
[147] Kim YH, Kumar SKS, Park Y, Kwon H, Kim C-G. High-velocity impact onto a high-frictional fabric treated with adhesive spray coating and shear thickening fluid impregnation. Composites Part B: Engineering. 2020:107742.
[148] Bajya M, Majumdar A, Butola BS, Verma SK, Bhattacharjee D. Design strategy for optimising weight and ballistic performance of soft body armour reinforced with shear thickening fluid. Composites Part B: Engineering. 2020;183:107721.
[149] Bai R, Ma Y, Lei Z, Feng Y, Liu C. Energy analysis of fabric impregnated by shear thickening fluid in yarn pullout test. Composites Part B: Engineering. 2019;174:106901.
[150] He Q, Cao S, Wang Y, Xuan S, Wang P, Gong X. Impact resistance of shear thickening fluid/Kevlar composite treated with shear-stiffening gel. Composites Part A: Applied Science and Manufacturing. 2018;106:82-90.
[151] Qin J, Guo B, Zhang L, Wang T, Zhang G, Shi X. Soft armor materials constructed with Kevlar fabric and a novel shear thickening fluid. Composites Part B: Engineering. 2020;183:107686.
[152] Majumdar A, Butola BS, Srivastava A. Development of soft composite materials with improved impact resistance using Kevlar fabric and nano-silica based shear thickening fluid. Materials & Design (1980-2015). 2014;54:295-300.
[153] Mawkhlieng U, Majumdar A. Deconstructing the role of shear thickening fluid in enhancing the impact resistance of high-performance fabrics. Composites Part B: Engineering. 2019;175:107167.
[154] Majumdar A, Laha A. Effects of fabric construction and shear thickening fluid on yarn pull-out from high-performance fabrics. Textile Research Journal. 2016;86:2056-66.
[155] Santos TF, Santos CM, Aquino MS, Oliveira FR, Medeiros JI. Statistical study of performance properties to impact of Kevlar® woven impregnated with Non-Newtonian Fluid (NNF). Journal of Materials Research and Technology. 2020;9:3330-9.
[156] Gong X, Xu Y, Zhu W, Xuan S, Jiang W, Jiang W. Study of the knife stab and puncture-resistant performance for shear thickening fluid enhanced fabric. Journal of Composite Materials. 2014;48:641-57.
[157] Zielinska D, Delczyk-Olejniczak B, Wierzbicki L, Wilbik-Hałgas Bże, Struszczyk MH, Leonowicz M. Investigation of the effect of para-aramid fabric impregnation with shear thickening fluid on quasi-static stab resistance. Textile Research Journal. 2014;84:1569-77.
[158] Xu Y, Chen X, Wang Y, Yuan Z. Stabbing resistance of body armour panels impregnated with shear thickening fluid. Composite Structures. 2017;163:465-73.
[159] Li W, Xiong D, Zhao X, Sun L, Liu J. Dynamic stab resistance of ultra-high molecular weight polyethylene fabric impregnated with shear thickening fluid. Materials & Design. 2016;102:162-7.
[160] Park Y, Kim Y, Baluch AH, Kim C-G. Empirical study of the high velocity impact energy absorption characteristics of shear thickening fluid (STF) impregnated Kevlar fabric. International Journal of Impact Engineering. 2014;72:67-74.
[161] Park Y, Kim Y, Baluch AH, Kim C-G. Numerical simulation and empirical comparison of the high velocity impact of STF impregnated Kevlar fabric using friction effects. Composite Structures. 2015;125:520-9.
[162] Wang Y, Li SK, Feng XY. The ballistic performance of multi-layer Kevlar fabrics impregnated with shear thickening fluids. Applied Mechanics and Materials: Trans Tech Publ; 2015. p. 153-7.

[163] Haro EE, Odeshi AG, Szpunar JA. The energy absorption behavior of hybrid composite laminates containing nano-fillers under ballistic impact. International Journal of Impact Engineering. 2016;96:11-22.
[164] Haris A, Lee H, Tay T, Tan V. Shear thickening fluid impregnated ballistic fabric composites for shock wave mitigation. International Journal of Impact Engineering. 2015;80:143-51.
[165] Talreja K, Chauhan I, Ghosh A, Majumdar A, Butola B. Functionalization of silica particles to tune the impact resistance of shear thickening fluid treated aramid fabrics. RSC Advances. 2017;7:49787-94.
[166] Tan V, Tay T, Teo W. Strengthening fabric armour with silica colloidal suspensions. International Journal of Solids and Structures. 2005;42:1561-76.
[167] Lee B-W, Kim C-G. Computational analysis of shear thickening fluid impregnated fabrics subjected to ballistic impacts. Advanced Composite Materials. 2012;21:177-92.
[168] Lee YS, Wetzel ED, Wagner NJ. The ballistic impact characteristics of Kevlar® woven fabrics impregnated with a colloidal shear thickening fluid. Journal of materials science. 2003;38:2825-33.
[169] Arora S, Majumdar A, Singh Butola B. Interplay of fabric structure and shear thickening fluid impregnation in moderating the impact response of high-performance woven fabrics. Journal of Composite Materials. 2020;54:4387-95.
[170] Mawkhlieng U, Majumdar A. Designing of hybrid soft body armour using high-performance unidirectional and woven fabrics impregnated with shear thickening fluid. Composite Structures. 2020;253:112776.
[171] Arora S, Majumdar A, Butola BS. Soft armour design by angular stacking of shear thickening fluid impregnated high-performance fabrics for quasi-isotropic ballistic response. Composite Structures. 2020;233:111720.
[172] Majumdar A, Laha A, Bhattacharjee D, Biswas I, Verma S. Soft body armour development by silica particle based shear thickening fluid coated p-aramid fabrics. The Journal of The Textile Institute. 2019;110:1515-8.
[173] Laha A, Majumdar A. Interactive effects of p-aramid fabric structure and shear thickening fluid on impact resistance performance of soft armor materials. Materials & Design. 2016;89:286-93.
[174] Arora S, Majumdar A, Butola BS. Structure induced effectiveness of shear thickening fluid for modulating impact resistance of UHMWPE fabrics. Composite Structures. 2019;210:41-8.
[175] Weerasinghe D, Mohotti D, Anderson J. Incorporation of shear thickening fluid effects into computational modelling of woven fabrics subjected to impact loading: A review. International Journal of Protective Structures. 2019:2041419619889071.
[176] Khodadadi A, Liaghat G, Sabet A, Hadavinia H, Aboutorabi A, Razmkhah O, et al. Experimental and numerical analysis of penetration into Kevlar fabric impregnated with shear thickening fluid. Journal of Thermoplastic Composite Materials. 2018;31:392-407.
[177] Hasanzadeh M, Mottaghitalab V, Rezaei M, Babaei H. Numerical and experimental investigations into the response of STF-treated fabric composites undergoing ballistic impact. Thin-Walled Structures. 2017;119:700-6.
[178] Gürgen S. Numerical modeling of fabrics treated with multi-phase shear thickening fluids under high velocity impacts. Thin-Walled Structures. 2020;148:106573.
[179] Rabb RJ, Fahrenthold EP. Simulation of large fragment impacts on shear-thickening fluid kevlar fabric barriers. Journal of aircraft. 2011;48:2059-67.
[180] Lu Z, Wu L, Gu B, Sun B. Numerical simulation of the impact behaviors of shear thickening fluid impregnated warp-knitted spacer fabric. Composites Part B: Engineering. 2015;69:191-200.
[181] Sen S, Shaw A, Deb A. Numerical investigation of ballistic performance of shear thickening fluid (STF)-Kevlar composite. International Journal of Mechanical Sciences. 2019;164:105174.
[182] Baharvandi HR, Alebooyeh M, Alizadeh M, Heydari MS, Kordani N, Khaksari P. The influences of particle–particle interaction and viscosity of carrier fluid on characteristics of

silica and calcium carbonate suspensions-coated Twaron® composite. Journal of Experimental Nanoscience. 2016;11:550-63.
[183] Ghosh A, Majumdar A, Butola BS. Rheometry of novel shear thickening fluid and its application for improving the impact energy absorption of p-aramid fabric. Thin-Walled Structures. 2020;155:106954.
[184] Liu L, Yang Z, Zhao Z, Liu X, Chen W. The influences of rheological property on the impact performance of kevlar fabrics impregnated with SiO2/PEG shear thickening fluid. Thin-Walled Structures. 2020;151:106717.
[185] Gürgen S. An investigation on composite laminates including shear thickening fluid under stab condition. Journal of Composite Materials. 2019;53:1111-22.
[186] Zarei M, Aalaie J. Application of shear thickening fluids in material development. Journal of Materials Research and Technology. 2020;9:10411-33.
[187] Galindo-Rosales FJ. Complex fluids in energy dissipating systems. Applied Sciences. 2016;6:206.
[188] Gürgen S, Fernandes FA, de Sousa RJA, Kuşhan MC. Development of Eco-friendly Shock-absorbing Cork Composites Enhanced by a Non-Newtonian Fluid. Applied Composite Materials. 2021;28:165-79.
[189] Gürgen S, Sofuoğlu MA. Vibration attenuation of sandwich structures filled with shear thickening fluids. Composites Part B: Engineering. 2020;186:107831.
[190] Gürgen S, Sofuoğlu MA. Smart polymer integrated cork composites for enhanced vibration damping properties. Composite Structures. 2021;258:113200.
[191] Cepero-Mejías F, Curiel-Sosa J, Blázquez A, Yu T, Kerrigan K, Phadnis V. Review of recent developments and induced damage assessment in the modelling of the machining of long fibre reinforced polymer composites. Composite Structures. 2020:112006.
[192] Andrew JJ, Srinivasan SM, Arokiarajan A, Dhakal HN. Parameters influencing the impact response of fiber-reinforced polymer matrix composite materials: a critical review. Composite Structures. 2019:111007.
[193] Abtew MA, Boussu F, Bruniaux P, Loghin C, Cristian I. Ballistic impact mechanisms-A review on textiles and fibre-reinforced composites impact responses. Composite Structures. 2019:110966.
[194] Patil NA, Mulik SS, Wangikar KS, Kulkarni AP. Characterization of glass laminate aluminium reinforced epoxy-A review. Procedia Manufacturing. 2018;20:554-62.
[195] Sivaraman R, Roseenid TA, Siddanth S. Reinforcement of elastomeric rubber using carbon fiber laminates. International Journal of Innovative Research in Science, Engineering and Technology. 2013;2:3123-30.
[196] Gamache R, Giller C, Montella G, Fragiadakis D, Roland C. Elastomer-metal laminate armor. Materials & Design. 2016;111:362-8.
[197] Kalpakjian S, Schmid S. Manufacturing engineering and technology. K. V. Sekar. Upper Saddle River; 2014.
[198] Zaman HU, Khan MA, Khan RA. Comparative experimental studies of phosphate glass fiber/polypropylene and phosphate glass fiber/natural rubber composites. Journal of Elastomers & Plastics. 2012;44:499-514.
[199] Dong Y, Ke Y, Zheng Z, Yang H, Yao X. Effect of stress relaxation on sealing performance of the fabric rubber seal. Composites Science and Technology. 2017;151:291-301.
[200] Khodadadi A, Liaghat G, Ahmadi H, Bahramian AR, Anani Y, Razmkhah O, et al. Numerical and experimental study of impact on hyperelastic rubber panels. Iranian Polymer Journal. 2019;28:113-22.
[201] Liaghat G, Ahmadi H, Anani Y. Experimental and Numerical Analysis of High Velocity Impact on 2-Layer kevlar/Elastomer Composite. Modares Mechanical Engineering. 2020;20:2733-45.
[202] Yang L, Shim V. A visco-hyperelastic constitutive description of elastomeric foam. International Journal of Impact Engineering. 2004;30:1099-110.

[203] Dong Y, Yao X, Yan H, Yuan L, Yang H. Macro-and mesoscopic mechanical properties of complex fabric rubber composite under different temperatures. Composite Structures. 2019;230:111510.
[204] Yang H, Yao X-F, Ke Y-C, Ma Y-j, Liu Y-H. Constitutive behaviors and mechanical characterizations of fabric reinforced rubber composites. Composite Structures. 2016;152:117-23.
[205] Dong Y, Yang H, Yan H, Yao X. Design and characteristics of fabric rubber sealing based on microchannel model. Composite Structures. 2019;229:111463.
[206] Yang H, Yao X-F, Yan H, Yuan Y-n, Dong Y-F, Liu Y-H. Anisotropic hyper-viscoelastic behaviors of fabric reinforced rubber composites. Composite Structures. 2018;187:116-21.
[207] Ahmad MR, Ahmad WYW, Salleh J, Samsuri A. Performance of natural rubber coated fabrics under ballistic impact. Malaysian Polymer Journal. 2007;2:39-51.
[208] Hassim N, Ahmad MR, Ahmad WYW, Samsuri A, Yahya MHM. Puncture resistance of natural rubber latex unidirectional coated fabrics. Journal of Industrial Textiles. 2012;42:118-31.
[209] Ahmad MR, Ahmad WYW, Samsuri A, Salleh J. Ballistic response of natural rubber latex coated and uncoated fabric systems. Journal of Rubber Research. 2007;10:207-21.
[210] Ahmad MR, Ahmad WYW, Salleh J, Samsuri A. Effect of fabric stitching on ballistic impact resistance of natural rubber coated fabric systems. Materials & Design. 2008;29:1353-8.
[211] Roy R, Laha A, Awasthi N, Majumdar A, Butola BS. Multi layered natural rubber coated woven P-aramid and UHMWPE fabric composites for soft body armor application. Polymer Composites. 2018;39:3636-44.
[212] Roy R, Majumdar A, Butola BS. Comparative study of P-aramid based soft and stiff composite panels for protective application. Fibers and Polymers. 2019;20:406-12.
[213] Mahesh V, Joladarashi S, Kulkarni SM. Influence of thickness and projectile shape on penetration resistance of the compliant composite. Defence Technology. 2020;17:245-256.
[214] Mahesh V, Joladarashi S, Kulkarni SM. Development and mechanical characterization of novel polymer-based flexible composite and optimization of stacking sequences using VIKOR and PSI techniques. Journal of Thermoplastic Composite Materials. 2019:0892705719864619.
[215] Mahesh V, Joladarashi S, Kulkarni SM. An experimental investigation on low-velocity impact response of novel jute/rubber flexible bio-composite. Composite Structures. 2019;225:111190.
[216] Mahesh V, Joladarashi S, Kulkarni SM. Damage mechanics and energy absorption capabilities of natural fiber reinforced elastomeric based bio composite for sacrificial structural applications. Defence Technology. 2020;17:161-176.
[217] Khodadadi A, Liaghat G, Ahmadi H, Bahramian AR, Razmkhah O. Impact response of Kevlar/rubber composite. Composites Science and Technology. 2019;184:107880.
[218] Hashemi SJ, Sadooghi A, Rahmani K, Nokbehrosta S. Experimental determining the mechanical and stiffness properties of natural rubber FRT triangle elastic joint composite reinforcement by glass fibers and micro/nano particles. Polymer Testing. 2020;85:106461.
[219] Stoll M, Stemmer F, Ilinzeer S, Weidenmann KA. Optimization of corrosive properties of carbon fiber reinforced aluminum laminates due to integration of an elastomer interlayer. Key Engineering Materials: Trans Tech Publ; 2017. p. 287-93.
[220] Stoll MM, Weidenmann KA. Materials selection for a fiber-metal-laminate with elastomer interlayers. roceedings of the 21st international conference on composite materials Xi'an; 2017.
[221] Stoll MM, Sessner V, Kramar M, Technau J, Weidenmann KA. The effect of an elastomer interlayer thickness variation on the mechanical properties of fiber-metal-laminates. Composite Structures. 2019;219:90-6.
[222] Stoll M, Weidenmann K. characterization of interface properties of Fiber-Metal-Laminates (FML) with optimized surfaces. Euro Hybrid Materials and Structures. 2016;38:43.

[223] Sessner V, Stoll M, Feuvrier A, Weidenmann KA. Determination of the damping characteristics of fiber-metal-elastomer laminates using piezo-indicated-loss-factor experiments. Key Engineering Materials: Trans Tech Publ; 2017. p. 325-32.
[224] Liebig WV, Sessner V, Weidenmann KA, Kärger L. Numerical and experimental investigations of the damping behaviour of hybrid CFRP-elastomer-metal laminates. Composite Structures. 2018;202:1109-13.
[225] Sarlin E, Liu Y, Vippola M, Zogg M, Ermanni P, Vuorinen J, et al. Vibration damping properties of steel/rubber/composite hybrid structures. Composite Structures. 2012;94:3327-35.
[226] Sarlin E, Heinonen E, Vuorinen J, Vippola M, Lepistö T. Adhesion properties of novel corrosion resistant hybrid structures. International Journal of Adhesion and Adhesives. 2014;49:51-7.
[227] Sarlin E, Hoikkanen M, Frisk L, Vuorinen J, Vippola M, Lepistö T. Ageing of corrosion resistant steel/rubber/composite hybrid structures. International Journal of Adhesion and Adhesives. 2014;49:26-32.
[228] Mehrizi MZ, Taherzadeh-Fard A, Liaghat G, Ahmadi H, Anani Y, Khodadadi A, et al. Experimental investigation on the inter-laminar strength in a hybrid elastomer modified fiber metal laminate under high and low velocity impact and quasi-static bending. Amirkabir J Mech Eng. 2019;52:181-90.
[229] Mohotti D, Ngo T, Mendis P, Raman SN. Polyurea coated composite aluminium plates subjected to high velocity projectile impact. Materials & Design (1980-2015). 2013;52:1-16.
[230] Mohotti D, Ngo T, Raman SN, Mendis P. Analytical and numerical investigation of polyurea layered aluminium plates subjected to high velocity projectile impact. Materials & Design. 2015;82:1-17.
[231] Xue L, Mock Jr W, Belytschko T. Penetration of DH-36 steel plates with and without polyurea coating. Mechanics of materials. 2010;42:981-1003.
[232] Bogoslovov R, Roland C, Gamache R. Impact-induced glass transition in elastomeric coatings. Applied physics letters. 2007;90:221910.
[233] Roland C, Fragiadakis D, Gamache R, Casalini R. Factors influencing the ballistic impact resistance of elastomer-coated metal substrates. Philosophical Magazine. 2013;93:468-77.
[234] Grujicic M, Pandurangan B, He T, Cheeseman B, Yen C-F, Randow C. Computational investigation of impact energy absorption capability of polyurea coatings via deformation-induced glass transition. Materials Science and Engineering: A. 2010;527:7741-51.
[235] Khodadadi A, Liaghat G, Shahgholian-Ghahfarokhi D, Chizari M, Wang B. Numerical and experimental investigation of impact on bilayer aluminum-rubber composite plate. Thin-Walled Structures. 2020;149:106673.
[236] Mohotti D, Ngo T, Raman SN, Ali M, Mendis P. Plastic deformation of polyurea coated composite aluminium plates subjected to low velocity impact. Materials & Design (1980-2015). 2014;56:696-713.
[237] Taherzadeh-Fard A, Liaghat G, Ahmadi H, Razmkhah O, Charandabi SC, Zarezadeh-mehrizi MA, khodadadi A. Experimental and numerical investigation of the impact response of elastomer layered fiber metal laminates (EFMLs). Composite Structures. 2020:112264.
[238] Sarlin E, Apostol M, Lindroos M, Kuokkala VT, Vuorinen J, Lepistö T, et al. Impact properties of novel corrosion resistant hybrid structures. Composite Structures. 2014;108:886-93.